The chiral Gaussian two-matrix ensemble of real asymmetric matrices

G. Akemann[1], M. J. Phillips[1], and H.-J. Sommers[2]

[1] *Department of Mathematical Sciences & BURSt Research Centre, Brunel University West London, Uxbridge UB8 3PH, United Kingdom*

[2] *Fakultät für Physik, Universität Duisburg-Essen, 47048 Duisburg, Germany*

Abstract. We solve a family of Gaussian two-matrix models with rectangular $N \times (N + \nu)$ matrices, having real asymmetric matrix elements and depending on a non-Hermiticity parameter μ. Our model can be thought of as the chiral extension of the real Ginibre ensemble, relevant for Dirac operators in the same symmetry class. It has the property that its eigenvalues are either real, purely imaginary, or come in complex conjugate eigenvalue pairs. The eigenvalue joint probability distribution for our model is explicitly computed, leading to a non-Gaussian distribution including K-Bessel functions. All n-point density correlation functions are expressed for finite N in terms of a Pfaffian form. This contains a kernel involving Laguerre polynomials in the complex plane as a building block which was previously computed by the authors. This kernel can be expressed in terms of the kernel for *complex* non-Hermitian matrices, generalising the known relation among ensembles of Hermitian random matrices. Compact expressions are given for the density at finite N as an example, as well as its microscopic large-N limits at the origin for fixed ν at strong and weak non-Hermiticity.

1. Introduction

Non-Hermitian Random Matrix Theory (RMT) introduced by Ginibre [1] is almost as old as its Hermitian counterpart. At first it was seen as an academic exercise to drop the Hermiticity constraint and thus to allow for complex eigenvalues. However, in the past two decades we have seen many applications of such RMTs featuring complex eigenvalues precisely for physical reasons, and we refer to [2] for examples and references. Because matrices with real data are often modelled by RMT one could view the real Ginibre ensemble of asymmetric matrices as being the most interesting non-Hermitian ensemble. Unfortunately it has also turned out to be the most difficult one, as it took over 25 years to compute the joint distribution of its eigenvalues [3, 4], being real or coming in complex conjugate pairs. The integrable structure and all eigenvalue correlation functions were computed only very recently for the real Ginibre ensemble [5, 6, 7, 8, 9, 10, 11].

Our motivation for generalising this model is as follows. In the 1990's Verbaarschot proposed extending the three classical (and Hermitian) ensembles of Wigner and Dyson to so-called chiral RMT [12], in order to describe the low energy sector of Quantum

Chromodynamics (QCD) and related field theories. These chiral ensembles are also known as Wishart or Laguerre ensembles. Their non-Hermitian extensions [13, 14] were motivated by adding a chemical potential for the quarks, which breaks the anti-Hermiticity of the Dirac operator in field theory. It was observed numerically quite early [14] that these chiral versions of the Ginibre ensembles have distinct features, either attracting eigenvalues to the real and imaginary axes (real matrices), repelling them (quaternion real matrices) or having no such symmetry (complex matrices). Only later was it realised how to solve these chiral non-Hermitian RMTs analytically, by using replicas [15] or by extending the initial one-matrix model plus a constant symmetry-breaking term [13, 14] to a two-matrix model. This idea from Osborn [16] led to a complex eigenvalue model that can be solved using orthogonal polynomials in the complex plane [17]. The solution of the two-matrix model was then derived for complex [16, 18] and quaternion real matrices [19]. Our paper aims to solve the third and most difficult of such non-Hermitian RMTs, a chiral two-matrix model of real asymmetric matrices introduced in our previous work [20]. For more details on RMT applications to the QCD-like Dirac operator spectrum we refer to [21].

Many more non-Hermitian RMTs than just the three Ginibre ensembles and their chiral (or Wishart/Laguerre) counterparts exist [22] and these are mostly unsolved to date. Very recently another two-matrix model generalisation of the real Ginibre ensembles was introduced and solved in [23]. There the eigenvalue correlations of the *ratio* of two quadratic matrices are sought, whereas here we deal with the *product* of two rectangular matrices. Whilst the former case leads to a Cauchy-type weight function, in our model we will obtain a weight of Bessel-K functions for the eigenvalues. We hope that given the plethora of RMT applications, our particular model will find applications beyond the field theory that it has been designed for.

The approach of solving our model is based on the variational method detailed in [7, 10]. It follows its two main ideas: first to compute the joint probability distribution function (jpdf) for general N by reducing it to 2×2 and 1×1 blocks. Because we are considering rectangular matrices this is *a priori* not guaranteed to work. Second, we use the variational method [7, 10] in combining all density correlations with n points (being real, purely imaginary or complex conjugates) into a single Pfaffian form. This reduces the computation to determining its main building block, an anti-symmetric kernel. Whilst it can be deduced from the spectral 1-point density – which was known for the real Ginibre ensemble [24] – we here exploit an idea from our previous publication [20]. There the kernel was determined by computing the expectation value of two characteristic polynomials using Grassmannians. The same relation between kernel and characteristic polynomials is known to hold for the symmetry classes with complex [25] or quaternion real matrices [19], in fact for any class of non-Gaussian weight functions.

As a new result we can express our kernel for real asymmetric matrices in terms of the kernel for complex non-Hermitian matrices. Such a relation might have been expected to exist as it is known for Hermitian RMT [26, 27].

Other methods that have been applied successfully to the real Ginibre ensemble such

as the supersymmetric method [28], skew-orthogonal polynomials [8] or probabilistic methods [9] are very likely to be extendible to our two-matrix model as well.

The paper is organised as follows. In Section 2 we summarise our main statements: the definition of the matrix model, its jpdf in terms of the real, imaginary and complex conjugate eigenvalue pairs, and the solution for all density correlation functions as a Pfaffian of a matrix-valued kernel. Examples are given for the simplest spectral densities at finite N and in the microscopic large-N limits for strong and for weak non-Hermiticity at the origin. These findings are then detailed in Section 3 on the jpdf, where we separately treat $N = 1, 2$ and general N. The spectral density correlations and their finite- and large-N results are derived and illustrated in Section 4. Our conclusions are presented in Section 5. Some technical details on the computation of the Jacobian are collected in Appendix A.

2. Summary of results

2.1. The model

The chiral Gaussian ensemble of real asymmetric matrices as introduced by the authors [20] is given by a two-matrix model of rectangular matrices P and Q of sizes $N \times (N+\nu)$ with real elements, without further symmetry restriction. The partition function normalised to unity is given by

$$\mathcal{Z} = \left(\frac{1}{\sqrt{2\pi}}\right)^{2N(N+\nu)} \int_{\mathbb{R}^{N(N+\nu)}} dP \int_{\mathbb{R}^{N(N+\nu)}} dQ \; \exp\left[-\frac{1}{2}\mathrm{Tr}(PP^T + QQ^T)\right] \;, \quad (2.1)$$

where we integrate over all the independent, normally distributed matrix elements of P and Q. We are interested in the eigenvalues of the matrix $\mathcal{D}$ of size $2N + \nu$ squared

$$\mathcal{D} \equiv \begin{pmatrix} 0 & P + \mu Q \\ P^T - \mu Q^T & 0 \end{pmatrix} \equiv \begin{pmatrix} 0 & A \\ B^T & 0 \end{pmatrix} \; . \quad (2.2)$$

Here $\mu \in (0, 1]$ is the non-Hermiticity parameter, interpolating between the chGOE ($\lim \mu \to 0$) and maximal non-Hermiticity ($\mu = 1$). The analogous chiral Gaussian two-matrix models with unitary and symplectic symmetry were introduced in [16, 19] respectively.

In applications to field theory, $\mathcal{D}$ corresponds to the chiral Dirac operator, and μ to the chemical potential‡. Typically, N_f extra determinants of the type $\det[\mathcal{D} + mI_{2N+\nu}]$ are inserted into the partition function eq. (2.1), where m is the quark mass, but we will restrict ourselves in this paper to the case $N_f = 0$; this is referred to as the quenched case.

For later convenience we give an equivalent form of eq. (2.1), by changing variables from

$$P = \frac{1}{2}(A + B) \; , \quad Q = \frac{1}{2\mu}(A - B) \; , \quad (2.3)$$

‡ The Euclidian Dirac operator in field theory is actually anti-Hermitian for $\mu = 0$, but we will not use this convention here.

to matrices A and B defined in eq. (2.2):

$$\mathcal{Z} = \left(\frac{1}{4\pi\mu}\right)^{N(N+\nu)} \int_{\mathbb{R}^{N(N+\nu)}} dA \int_{\mathbb{R}^{N(N+\nu)}} dB \; \mathrm{e}^{-\frac{1}{2}\eta_+ \mathrm{Tr}(AA^T+BB^T)+\frac{1}{2}\eta_- \mathrm{Tr}(AB^T+BA^T)} \;, \tag{2.4}$$

$$\text{with} \;\; \eta_\pm \;\equiv\; \frac{1\pm\mu^2}{4\mu^2} \;. \tag{2.5}$$

The two μ-dependent combinations $\eta_\pm$ will be used throughout the paper.

2.2. Eigenvalue representation

The eigenvalues Λ of the Dirac matrix $\mathcal{D}$ are determined from the following equation§:

$$0 = \det[\Lambda I_{2N+\nu} - \mathcal{D}] = \Lambda^\nu \det[\Lambda^2 I_N - AB^T] = \Lambda^\nu \prod_{j=1}^{N} (\Lambda^2 - \Lambda_j^2) \;. \tag{2.6}$$

For this reason we will first compute the eigenvalue distribution of the $N \times N$ Wishart-type combination of matrices $C \equiv AB^T$. C has real elements, and therefore its eigenvalues Λ_j^2 are real, or else come in complex conjugate pairs. The matrix $\mathcal{D}$ itself has the following solutions: ν zero-eigenvalues $\Lambda = 0$, and $2N$ eigenvalues coming in pairs $\Lambda = \pm\Lambda_j$. Consequently the non-zero eigenvalues of $\mathcal{D}$ fall into three categories:

(i) for $\Lambda_j^2 > 0$: real pairs $\Lambda = \pm\Lambda_j \in \mathbb{R}$

(ii) for $\Lambda_j^2 < 0$: purely imaginary pairs $\Lambda = \pm\Lambda_j \in i\mathbb{R}$

(iii) for pairs $\Lambda_j^2, \Lambda_j^{*\,2}$: quadruplets $\Lambda = \pm\Lambda_j, \pm\Lambda_j^* \in \mathbb{C} \setminus \{\mathbb{R} \cup i\mathbb{R}\}$.

This leads to an accumulation of eigenvalues on both the real and the imaginary axes as already pointed out in [20]. The same phenomenon has been observed numerically in a one-matrix model [14] based on the proposal [13] (obtained from eq. (2.1) by choosing $Q \sim I$). This is in contrast to the real Ginibre model where eigenvalues accumulate only on the real axis (see e.g. [29]).

The joint probability distribution (jpdf) for the matrix C is obtained from eq. (2.4) by inserting a matrix delta function; using the cyclic property of the trace we then have

$$P(C) \sim \exp[\eta_- \mathrm{Tr}\, C] \int_{\mathbb{R}^{N(N+\nu)}} dA \int_{\mathbb{R}^{N(N+\nu)}} dB \exp\left[-\frac{\eta_+}{2}\mathrm{Tr}(AA^T + BB^T)\right] \delta(C - AB^T) \;. \tag{2.7}$$

As shown in Section 3, our final result for the jpdf of $\mathcal{D}$ in terms of squared variables $z_k = x_k + iy_k \equiv \Lambda_k^2$ with $d^2 z_k = dx_k dy_k$ is

$$\mathcal{Z} = \int_{\mathbb{C}} d^2 z_1 \ldots \int_{\mathbb{C}} d^2 z_N P_N(z_1, \ldots, z_N) \tag{2.8}$$

$$= c_N \prod_{k=1}^{N} \int_{\mathbb{C}} d^2 z_k \, w(z_k) \prod_{i<j}^{N} (z_i - z_j) \sum_{n=0}^{[N/2]} \Big(\prod_{l=1}^{n} (-2i)\delta(x_{2l-1} - x_{2l})\delta(y_{2l-1} + y_{2l})\Theta(y_{2l-1}) \times \Theta(x_1 > x_3 > \ldots > x_{2n-1})\Theta(x_{2n+1} > x_{2n+2} > \ldots > x_N)\delta(y_{2n+1})\ldots\delta(y_N)\Big). \tag{2.9}$$

§ This follows from eq. (2.2) using the standard relation $\det \begin{pmatrix} a & b \\ c & d \end{pmatrix} = \det(d)\, \det(a - bd^{-1}c)$ for square matrices a and d, with d invertible.

The integration measure d^2z_k extends over the complex plane for *each* of the z_k. The normalisation constant c_N will be given in eq. (3.46). In eq. (2.9) we sum over all distinct possibilities for N eigenvalues to come in $n \geq 0$ complex conjugate pairs, with the remaining $N - 2n \geq 0$ eigenvalues being real. For $n = 0$ in eq. (2.9) the product in the first line is simply unity.

Specifically, the jpdf is only non-zero when the eigenvalues appear in the following order: the n complex eigenvalue pairs must be placed first, ordered with respect to decreasing real parts‖

$$(\Im\mathrm{m}\Lambda_1^2 > 0),\ (\Re\mathrm{e}\Lambda_2^2 = \Re\mathrm{e}\Lambda_1^2, \Im\mathrm{m}\Lambda_2^2 = -\Im\mathrm{m}\Lambda_1^2),\ (\Re\mathrm{e}\Lambda_3^2 \leq \Re\mathrm{e}\Lambda_2^2, \Im\mathrm{m}\Lambda_3^2 > 0), \ldots,$$
$$(\Re\mathrm{e}\Lambda_{2n-1}^2 \leq \Re\mathrm{e}\Lambda_{2n-2}^2, \Im\mathrm{m}\Lambda_{2n-1}^2 > 0),\ (\Re\mathrm{e}\Lambda_{2n}^2 = \Re\mathrm{e}\Lambda_{2n-1}^2, \Im\mathrm{m}\Lambda_{2n}^2 = -\Im\mathrm{m}\Lambda_{2n-1}^2), \quad (2.10)$$

and the $N - 2n \geq 0$ real eigenvalues follow, and are also ordered with respect to decreasing real parts:

$$\Lambda_{2n+1}^2 > \Lambda_{2n+2}^2 > \ldots > \Lambda_N^2 \ . \quad (2.11)$$

The function $g(z)$ inside the weight function

$$w(z) \equiv |z|^{\nu/2} \exp[\eta_- z]\, g(z) \quad (2.12)$$

depends on whether $z\,(\equiv \Lambda^2)$ is real or complex:

$$g(z) \quad \equiv 2K_{\frac{\nu}{2}}(\eta_+|z|)\ ,\ \text{for}\ \ z \in \mathbb{R}\ , \quad (2.13)$$

$$[g(z)]^2 \ = \ [g(z^*)]^2 \equiv 2\int_0^\infty \frac{dt}{t} \mathrm{e}^{-2\eta_+^2 t(x^2-y^2)-\frac{1}{4t}} K_{\frac{\nu}{2}}\left(2\eta_+^2 t(x^2+y^2)\right) \mathrm{erfc}(2\eta_+\sqrt{t}|y|), \quad (2.14)$$
$$\text{for } z = x + iy \in \mathbb{C}.$$

Because the complex eigenvalues come in pairs we will always get *two* factors $g(z)$ for each pair (note the square on the left hand side of the definition eq. (2.14)). The limit $y \to 0$ of a single $g(z)$ in eq. (2.14) is smooth, leading to eq. (2.13).

The essential idea in the derivation of the jpdf detailed in Section 3 is to reduce the calculation of the jpdf for $\mathcal{D}$ with general N down to 2×2 and 1×1 blocks, which can be handled in terms of the $N = 2$ and $N = 1$ problems which we solve explicitly.

2.3. Density correlation functions for finite N

We follow the method of using a generating functional for all eigenvalue density correlation functions introduced in [7, 10]. Because we essentially follow [7, 10] we can be brief here. We enlarge the definition of the partition function eq. (2.9) by introducing sources $f(\Lambda_k^2)$:¶

$$\mathcal{Z}[f] \equiv \int_{\mathbb{C}} d^2z_1 \ldots \int_{\mathbb{C}} d^2z_N P_N(z_1, \ldots, z_N) f(z_1) \ldots f(z_N)\ . \quad (2.15)$$

‖ Unlike for real eigenvalues two complex eigenvalues that are not complex conjugates can have the same real part, without the jpdf vanishing. Although being of measure zero we can fix this ambiguity by ordering with respect to decreasing absolute imaginary part.

¶ These will symmetrise the ordered eigenvalues when differentiating.

For pairwise distinct arguments $z_1 \neq z_2 \neq \ldots \neq z_n$ the n-point density correlation functions are then generated in terms of functional derivatives with respect to the sources, leading to insertions of delta functions $\frac{\delta f(z)}{\delta f(z')} = \delta^2(z - z')$:

$$R_n(z_1, \ldots, z_n) = \frac{\delta}{\delta f(z_1)} \ldots \frac{\delta}{\delta f(z_n)} \mathcal{Z}[f]\Big|_{f\equiv 1} \ . \tag{2.16}$$

In doing so, each n-point function contains a sum of different contributions, splitting n into all possible combinations of real eigenvalues and complex eigenvalue pairs. Both the generating functional $\mathcal{Z}[f]$ and the n-point density R_n can be written as Pfaffians [6, 7]:

$$\mathcal{Z}[f] = c_N \ \mathrm{Pf}\left[\int_{\mathbb{C}} d^2 z_1 \int_{\mathbb{C}} d^2 z_2 \, f(z_1) f(z_2) \mathcal{F}(z_1, z_2) z_1^{i-1} z_2^{j-1}\right]_{1\leq i,j\leq N}, \tag{2.17}$$

$$\begin{aligned} R_n(z_1, \ldots, z_n) &\equiv \frac{N!}{(N-n)!} \int_{\mathbb{C}} d^2 z_{n+1} \ldots \int_{\mathbb{C}} d^2 z_N P_N(z_1, \ldots, z_N) \\ &= \mathrm{Pf} \begin{bmatrix} \mathcal{K}_N(z_i, z_j) & -G_N(z_i, z_j) \\ G_N(z_j, z_i) & -W_N(z_i, z_j) \end{bmatrix}_{1\leq i,j\leq n} . \end{aligned} \tag{2.18}$$

In the latter case, one has to compute the Pfaffian of the ordinary, $2n \times 2n$ matrix composed of the matrix of quaternions inside the square bracket. We have restricted ourselves to even N for simplicity. The case of odd N can be treated along the lines of [10] (or [11] for an alternative formulation). We have introduced the following functions of two complex variables $z_j = x_j + iy_j$, $j = 1, 2$:

$$\mathcal{F}(z_1, z_2) = w(z_1) w(z_2) \Big(2i\delta^2(z_1 - z_2^*) \mathrm{sgn}(y_1) + \delta(y_1)\delta(y_2)\mathrm{sgn}(x_2 - x_1) \Big), \tag{2.19}$$

$$\begin{aligned} \mathcal{K}_N(z_1, z_2) &= \frac{\eta_-}{8\pi(4\mu^2\eta_+)^{\nu+1}} \\ &\quad \times \sum_{j=0}^{N-2} \left(\frac{\eta_-}{\eta_+}\right)^{2j} \frac{(j+1)!}{(j+\nu)!} \left\{ L_{j+1}^{\nu}\Big(\frac{z_2}{4\mu^2\eta_-}\Big) L_j^{\nu}\Big(\frac{z_1}{4\mu^2\eta_-}\Big) - (z_1 \leftrightarrow z_2) \right\} \end{aligned} \tag{2.20}$$

$$\begin{aligned} &= \frac{\eta_-}{8\pi(4\mu^2\eta_+)^{\nu+1}} \left(z_2 \frac{\partial}{\partial z_2} - z_1 \frac{\partial}{\partial z_1} - \frac{z_2 - z_1}{4\mu^2\eta_-} \right) \\ &\quad \times \sum_{j=0}^{N-2} \left(\frac{\eta_-}{\eta_+}\right)^{2j} \frac{j!}{(j+\nu)!} L_j^{\nu}\Big(\frac{z_1}{4\mu^2\eta_-}\Big) L_j^{\nu}\Big(\frac{z_2}{4\mu^2\eta_-}\Big), \end{aligned} \tag{2.21}$$

$$G_N(z_1, z_2) = -\int_{\mathbb{C}} d^2 z \, \mathcal{K}_N(z_1, z) \mathcal{F}(z, z_2) \ , \tag{2.22}$$

$$W_N(z_1, z_2) = -\mathcal{F}(z_1, z_2) + \int_{\mathbb{C}} d^2 z \int_{\mathbb{C}} d^2 z' \mathcal{F}(z_1, z) \mathcal{K}_N(z, z') \mathcal{F}(z', z_2) \ . \tag{2.23}$$

The kernel $\mathcal{K}_N(z_1, z_2)$ is the building block of all correlations, and is actually defined in terms of $\mathcal{F}(z_1, z_2)$ (see Section 4 for further details). However, we will give a different proof of the precise form of eq. (2.20) which does not rely on direct evaluation of the definition; rather, it will be calculated from the expectation value of two characteristic polynomials (see also [20]). Note that in eq. (2.21) we have expressed the kernel of our

real two-matrix model ($\beta = 1$) as a derivative of the kernel of the complex two-matrix model [16] ($\beta = 2$). We found that a similar relation holds relating the kernel of the $\beta = 1$ real Ginibre ensemble [8, 20] to the one for the $\beta = 2$ complex Ginibre ensemble [30], containing Hermite polynomials in the complex plane.

There is an integration theorem in analogy to other matrix models with complex eigenvalues [7, 31, 26]:

$$\begin{aligned}&\int_{\mathbb{C}} d^2z_n \mathrm{Pf}\begin{bmatrix} \mathcal{K}_N(z_i,z_j) & -G_N(z_i,z_j) \\ G_N(z_j,z_i) & -W_N(z_i,z_j)\end{bmatrix}_{1\le i,j\le n} \\ &= (N-n+1)\mathrm{Pf}\begin{bmatrix} \mathcal{K}_N(z_i,z_j) & -G_N(z_i,z_j) \\ G_N(z_j,z_i) & -W_N(z_i,z_j)\end{bmatrix}_{1\le i,j\le n-1} . \end{aligned} \tag{2.24}$$

This is the major advantage of working with an n-point correlation function as defined in eq. (2.18) which contains all possible contributions of real eigenvalues and complex conjugate eigenvalue pairs. Had we studied instead a particular n-point function with a fixed and given number of real and complex conjugate eigenvalues, then we would have found that such a simple integration theorem does not exist [5].

Let us spell out one example explicitly, the spectral density, which we will give for even N only. Details can be found in Section 4 including figures, where we follow the method of [7, 10]. From eq. (2.18) we have

$$R_1(z_1) = \int_{\mathbb{C}} d^2z\, \mathcal{K}_N(z_1,z)\mathcal{F}(z,z_1) \equiv R_1^{\mathbb{C}}(z_1) + \delta(y_1) R_1^{\mathbb{R}}(x_1) \ . \tag{2.25}$$

Inserting the appropriate weight from eqs. (2.13) and (2.14) we obtain with $z = x + iy$

$$\begin{aligned} R_1^{\mathbb{C}}(z) =& -2i|z|^\nu \mathrm{e}^{2\eta_- x}\mathrm{sgn}(y)\mathcal{K}_N(z,z^*) \\ &\times 2\int_0^\infty \frac{dt}{t}\exp\Big[-2\eta_+^2 t(x^2-y^2) - \frac{1}{4t}\Big] K_{\frac{\nu}{2}}\Big(2\eta_+^2 t(x^2+y^2)\Big)\mathrm{erfc}\left(2\eta_+\sqrt{t}|y|\right), \end{aligned} \tag{2.26}$$

$$R_1^{\mathbb{R}}(x) = \int_{-\infty}^{\infty} dx' \mathrm{sgn}(x-x')\,|xx'|^{\frac{\nu}{2}}\mathrm{e}^{\eta_-(x+x')} 2K_{\frac{\nu}{2}}(\eta_+|x|)2K_{\frac{\nu}{2}}(\eta_+|x'|)\,\mathcal{K}_N(x,x'). \tag{2.27}$$

Eqs. (2.25) – (2.27) are valid for even N only. In the final step we can change from squared variables $z = x + iy = \Lambda^2$ to Dirac eigenvalues Λ, using the simple transformations

$$\begin{aligned} R_{1\,Dirac}^{\mathbb{C}}(z) &= 4|z|^2 R_1^{\mathbb{C}}(z^2), \\ R_{1\,Dirac}^{\mathbb{R}}(x) &= 2|x| R_1^{\mathbb{R}}(x^2). \end{aligned} \tag{2.28}$$

Note that the latter describes the density both of real Dirac eigenvalues, for $R_{1\,Dirac}^{\mathbb{R}}(x)$ with $x \in \mathbb{R}$, and of purely imaginary Dirac eigenvalues, for $R_{1\,Dirac}^{\mathbb{R}}(x)$ with $x \in i\,\mathbb{R}$. Because $R_1^{\mathbb{R}}(x^2) \neq R_1^{\mathbb{R}}(-x^2)$ this is not the same function, see e.g. Fig. 2 in Section 4.

2.4. The large-N limit

In order to take the large-N limit in principle one first has to rescale all eigenvalues in eq. (2.9) $\Lambda_k \to \sqrt{N}\,\Lambda_k$, which is equivalent to giving all the matrix elements in eq. (2.1)

Gaussian weights $\exp[-(N/2)\mathrm{Tr}P^TP]$ for P, and similarly for Q. In this parametrisation the macroscopic spectral density will have a compact support in the large-N limit, given by a circle for $\mu = 1$, and an ellipse for $0 < \mu < 1$. We will not discuss this macroscopic limit in detail but will focus on the local correlations, i.e. the microscopic large-N limit. Here one has to distinguish between strong and weak non-Hermiticity [32], each of which involves a second rescaling.

We first give the strong non-Hermiticity limit *after* the first rescaling, defined by keeping μ fixed and only rescaling the eigenvalues according to

$$\lim_{N\to\infty,\Lambda\to 0} N\Lambda^2 \equiv \lambda^2 \ . \tag{2.29}$$

This scaling actually cancels the first scaling. Because of this the scaling limit is also true away from the origin.

We only give the microscopic kernel here, to be inserted into eqs. (2.26) and (2.27). For $\mu = 1$ the kernel simplifies to monic powers, see eq. (33) in [20]. Its large-N limit is easily seen to lead to a modified Bessel function

$$\mathcal{K}^S_\nu(z_1,z_2) = \frac{(z_1-z_2)}{64\pi 2^\nu}\sum_{j=0}^\infty \frac{1}{j!(j+\nu)!}\left(\frac{z_1z_2}{4}\right)^j = \frac{(z_1-z_2)}{64\pi}(z_1z_2)^{-\nu/2}I_\nu(\sqrt{z_1z_2}). \tag{2.30}$$

Because μ is not scaled here, in contrast to the weak limit below, the insertion into eqs. (2.26) and (2.27) is relatively straightforward, apart from the phase for negative real eigenvalues. The case for general μ which can also be obtained by simply rescaling the arguments in eq. (2.30) is discussed in Section 4 where we also show plots.

The weak non-Hermiticity limit at the origin (again *after* the initial rescaling above) is defined by scaling both the squared Dirac eigenvalues Λ^2 and the chemical potential μ^2 with $2N$, corresponding to the volume in field theory:

$$\lim_{N\to\infty,\mu\to 0} 2N\mu^2 \equiv \alpha^2 \ , \quad \lim_{N\to\infty,\Lambda\to 0}(2N)^2\Lambda^2 \equiv \lambda^2 \ . \tag{2.31}$$

In this limit the macroscopic density is projected back onto the real axis, with probability density given by the semi-circle as for $\mu = 0$ (when our model is Hermitian), whilst microscopically the eigenvalues still extend into the complex plane.

The limiting microscopic kernel, as a function of squared variables $z = \Lambda^2$, can be expressed in terms of our completely unscaled finite-N kernel as

$$\begin{aligned}\mathcal{K}^W(z_1,z_2) &\equiv \lim_{N\to\infty}\left[\frac{1}{(4N)^2}\left(\frac{z_1z_2}{(4N)^2}\right)^{\nu/2}\mathcal{K}_N\left(\frac{z_1}{4N},\frac{z_2}{4N};\mu=\frac{\alpha}{\sqrt{2N}}\right)\right] \\ &= \frac{1}{256\pi\alpha^2}\int_0^1 ds\, s^2\,\mathrm{e}^{-2\alpha^2s^2}\,\{\sqrt{z_1}\,J_{\nu+1}(s\sqrt{z_1})J_\nu(s\sqrt{z_2})-(z_1\leftrightarrow z_2)\}\end{aligned} \tag{2.32}$$

which is to be inserted into the definition of the density eq. (2.25). From eq. (2.26) we obtain for the microscopic density of complex eigenvalues

$$\begin{aligned}\rho^{\mathbb{C}\,W}_\nu(z) = &-2i\ \mathrm{sgn}(y)\ \exp\left[\frac{x}{4\alpha^2}\right]\mathcal{K}^W(z,z^*) \\ &\times 2\int_0^\infty\frac{dt}{t}\exp\Big[-\frac{t(x^2-y^2)}{32\alpha^4}-\frac{1}{4t}\Big]K_{\frac{\nu}{2}}\left(\frac{t(x^2+y^2)}{32\alpha^4}\right)\mathrm{erfc}\Big(\frac{\sqrt{t}|y|}{4\alpha^2}\Big).\end{aligned} \tag{2.33}$$

The real eigenvalue density is more subtle; we again refer to Section 4 for a more detailed discussion of the weak limit, including figures.

3. Calculation of the joint probability distribution function

In this section we compute the joint probability density function (jpdf) as stated in eq. (2.9) for the squared non-zero eigenvalues of $\mathcal{D}$. For pedagogical reasons we first compute the jpdf separately for $N = 1$ and 2 in Sections 3.1 and 3.2 respectively. This is because we will need these results when treating the general N case in Section 3.3, as these sub-blocks will appear in the computation of the general Jacobian. Some technical details will be deferred to Appendix A. The cases with $N = 1, 2$ will make the parametrisation and residual symmetries more transparent for later.

3.1. The $N = 1$ case

In this simplest case our matrices P and Q, or after changing variables A and B in eq. (2.3), are of size $1 \times (1+\nu)$ and are thus given by vectors $\mathbf{a}$ and $\mathbf{b}$, each of length $\nu+1$. The eigenvalue equation (2.6) for $\mathcal{D}$ becomes

$$0 = \Lambda^\nu(\Lambda^2 - \mathbf{a}\cdot\mathbf{b}) \,, \tag{3.1}$$

and thus we only have a single non-zero (and real) eigenvalue Λ^2 to determine. Its (j)pdf is given by

$$P(\Lambda^2) = \frac{1}{(4\pi\mu)^{\nu+1}} \int_{\mathbb{R}^{\nu+1}} d\mathbf{a} \int_{\mathbb{R}^{\nu+1}} d\mathbf{b}\, \exp[\eta_- \mathbf{a}\cdot\mathbf{b}] \exp\left[-\frac{\eta_+}{2}\left(|\mathbf{a}|^2 + |\mathbf{b}|^2\right)\right] \delta(\Lambda^2 - \mathbf{a}\cdot\mathbf{b}) \,. \tag{3.2}$$

We simplify this expression in two steps. First, without loss of generality we may choose the direction of $\mathbf{b}$ as the first basis vector for $\mathbf{a}$ in Cartesian coordinates. This leads to a decoupling of the remaining components $a_2, \ldots, a_{\nu+1}$, and the integral now only depends on $\mathbf{b}$ through its modulus $b = |\mathbf{b}|$. Second, we choose polar coordinates for the vector $\mathbf{b}$, leading to the Jacobian b^ν, and, on symmetrically extending the integral over b to $-\infty$, we obtain

$$\begin{aligned} P(\Lambda^2) &= \frac{1}{(4\pi\mu)^{\nu+1}} \frac{2\pi^{(\nu+1)/2}}{\Gamma\left(\frac{\nu+1}{2}\right)} \left(\frac{2\pi}{\eta_+}\right)^{\nu/2} \mathrm{e}^{\eta_-\Lambda^2} \frac{1}{2} \int_{-\infty}^{\infty} da_1 \int_{-\infty}^{\infty} db\, \mathrm{e}^{-\frac{1}{2}\eta_+(a_1^2+b^2)} \delta(\Lambda^2 - a_1 b)\, |b|^\nu \\ &= \frac{1}{2^{3\nu/2+2}\mu^{\nu+1}\eta_+^{\nu/2}\sqrt{\pi}\,\Gamma\left(\frac{\nu+1}{2}\right)} \mathrm{e}^{\eta_-\Lambda^2} \int_{-\infty}^{\infty} db\, \mathrm{e}^{-\frac{1}{2}\eta_+(b^2+\Lambda^4/b^2)}\, |b|^{\nu-1}. \end{aligned} \tag{3.3}$$

The first new pre-factor comes from the surface area of the unit ν-sphere

$$S_\nu \equiv \frac{2\pi^{(\nu+1)/2}}{\Gamma\left(\frac{\nu+1}{2}\right)} \;=\; \frac{VO(\nu+1)}{VO(\nu)} \tag{3.4}$$

(with $VO(\nu)$ being the volume of the orthogonal group) through the angular integration over $\mathbf{b}$, the final pre-factor from the Gaussian integrations over the decoupled components of $\mathbf{a}$. It is important to note that the first line of eq. (3.3) looks like a reduction to the $\nu = 0$ case, apart from the extra factor $|b|^\nu$ from the Jacobian. We will

use the same strategy for $N = 2$ in the following subsection. In the next step we change variables $\mathrm{e}^t = b^2/|\Lambda^2|$ to arrive at

$$P(\Lambda^2) = \frac{1}{2^{3\nu/2+2}\mu^{\nu+1}\eta_+^{\nu/2}\sqrt{\pi}\,\Gamma\left(\frac{\nu+1}{2}\right)}|\Lambda|^\nu \mathrm{e}^{\eta_-\Lambda^2}\, 2\int_0^\infty \cosh(\nu t/2)\mathrm{e}^{-\eta_+|\Lambda^2|\cosh t}\,dt$$
$$= \frac{1}{2^{3\nu/2+2}\mu^{\nu+1}\eta_+^{\nu/2}\sqrt{\pi}\,\Gamma\left(\frac{\nu+1}{2}\right)}|\Lambda|^\nu \mathrm{e}^{\eta_-\Lambda^2}\, 2\,K_{\frac{\nu}{2}}(\eta_+|\Lambda^2|)\ . \tag{3.5}$$

Here we have used a particular representation eq. 9.6.24 in [33] of the K-Bessel function. It directly gives $c_{N=1}$ times the weight function in eqs. (2.12) and (2.13) when changing variables $\Lambda^2 \to z$, where

$$c_{N=1} = \frac{1}{2\pi}\,\frac{1}{(2\pi)^{\nu/2}(2\mu)^{\nu+1}\eta_+^{\nu/2}}\,\frac{S_\nu}{S_0}. \tag{3.6}$$

This is consistent with eqs. (2.9), (2.12) and (2.13), and ends our calculation for $N = 1$.

As a remark, eq. (3.5) can be derived in various different ways, including by Fourier transformation. It is known that if a and b are independent random variables with normal distributions, then the product $c = ab$ has distribution function $P_0 \sim K_0$. Consequently, the sum of $\nu + 1$ (independent) such variables c_i has a distribution given by the convolution of $\nu + 1$ functions K_0. Fourier transformation F turns this into an ordinary product, and so we obtain $P_\nu = F^{-1}\left\{(F(P_0))^{\nu+1}\right\} \sim K_{\frac{\nu}{2}}$, i.e. on performing the integrals we again reach eq. (3.5).

3.2. The $N = 2$ case

Our matrices A and B are now given by two row vectors $\mathbf{a}_{j=1,2}$ and $\mathbf{b}_{j=1,2}$ each of length $\nu + 2$:

$$A = \begin{pmatrix} \mathbf{a}_1 \\ \mathbf{a}_2 \end{pmatrix}\ ,\quad B = \begin{pmatrix} \mathbf{b}_1 \\ \mathbf{b}_2 \end{pmatrix}\ ,\quad C = AB^T = \begin{pmatrix} \mathbf{a}_1\cdot\mathbf{b}_1 & \mathbf{a}_1\cdot\mathbf{b}_2 \\ \mathbf{a}_2\cdot\mathbf{b}_1 & \mathbf{a}_2\cdot\mathbf{b}_2 \end{pmatrix}. \tag{3.7}$$

The eigenvalue equation (2.6)

$$0 = \Lambda_\nu \det[\Lambda^2 I_2 - AB^T] \tag{3.8}$$

has two solutions $\Lambda^2_{1,2}$ which may (i) both be real or (ii) form a complex conjugate pair. We will have to distinguish these two cases below.

For the first step we reduce the calculation of $P(C)$ in eq. (2.7) to a matrix integral of 2×2 matrices A' and B' times a Jacobian, as we did for $N = 1$ in the first line of eq. (3.3). The resulting Jacobian here will be $\sim |\det B'|^\nu$. Our aim is to rotate both $\mathbf{b}_1$ and $\mathbf{b}_2$ into the xy-plane of the coordinates for the $\mathbf{a}_j$, as then

$$\mathbf{a}_i\cdot\mathbf{b}_j = \sum_{k=1}^{\nu+1} a_{ik}b_{jk} = a_{i1}b'_{j1} + a_{i2}b'_{j2}\ , \tag{3.9}$$

and the remaining components of the $\mathbf{a}_j$ decouple. Here we use primed vectors and coordinates to denote the quantities after rotation.

For $\nu = 1$ the corresponding Jacobian is obtained as follows. Rotating the 3D vector into 2D by $\mathbf{b}'_1 = O\,\mathbf{b}_1$ gives rise to a factor $\sim |\mathbf{b}_1|$. Alternatively it can be computed by comparing the initial and final 'volumes' (generalised surface areas, in fact), yielding $\frac{S_2|\mathbf{b}_1|^2}{S_1|\mathbf{b}_1|} = 2|\mathbf{b}_1|$, where S_n is given by eq. (3.4). The remaining rotation around $\mathbf{b}_1$ rotates $\mathbf{b}_2$ into the xy-plane as well, giving $\frac{S_1|\mathbf{b}_2|\sin\theta}{S_0} = \pi|\mathbf{b}_2|\sin\theta$, in which $\theta \in [0,\pi]$ is the angle between $\mathbf{b}_1$ and $\mathbf{b}_2$. The final Jacobian reads

$$|\mathbf{b}_1|\,|\mathbf{b}_2|\sin\theta = |\mathbf{b}'_1|\,|\mathbf{b}'_2|\sin\theta = \begin{vmatrix} b'_{11} & b'_{12} \\ b'_{21} & b'_{22} \end{vmatrix} = |\det B'|\ , \tag{3.10}$$

where the last equality easily follows by parametrising $\mathbf{b}'_1$ and $\mathbf{b}'_2$ in 2D, and the factor $\frac{S_2}{S_0}$ corresponds to the angular integration over $\mathbf{b}$.

For $\nu > 1$ we can thus successively repeat these steps by projecting onto one dimension lower until we reach the xy-plane. The volume factors will telescope out and we arrive at

$$\frac{S_\nu S_{\nu+1}}{S_0 S_1}(|\mathbf{b}'_1||\mathbf{b}'_2|\sin\theta)^\nu = \frac{S_\nu S_{\nu+1}}{S_0 S_1}|\det B'|^\nu. \tag{3.11}$$

We thus have reduced eq. (2.7) for $N = 2$ from $2\times(2+\nu)$ down to 2×2 matrices:

$$\begin{aligned} P(C) = {} & \frac{c_{N=2}\,\eta_+}{2\pi^3}\,\mathrm{e}^{\eta_-\mathrm{Tr}\,C} \\ & \times \int_{\mathbb{R}^4} dA' \int_{\mathbb{R}^4} dB'\ \exp\left[-\frac{1}{2}\eta_+\mathrm{Tr}(A'A'^T + B'B'^T)\right]\delta\left(C - A'B'^T\right)\,|\det B'|^\nu\ , \end{aligned} \tag{3.12}$$

where $c_{N=2}$ is defined in anticipation of the final result as

$$c_{N=2} = \frac{1}{8\pi}\,\frac{1}{(2\pi)^\nu(2\mu)^{4+2\nu}\eta_+^{\nu+1}}\,\frac{S_\nu S_{\nu+1}}{S_0 S_1}. \tag{3.13}$$

The Gaussian integrals over the decoupled components of the two vectors a_{jk} for $k > 2$ have been evaluated, using that $\mathrm{Tr}AA^T = |\mathbf{a}_1|^2 + |\mathbf{a}_2|^2$. The 2×2 matrix A' can now be integrated out, by formally changing variables $A' \to F = A'B'^T$ with Jacobian $|\det B'|^{-2}$:

$$P(C) = \frac{c_{N=2}\,\eta_+}{2\pi^3}\,\mathrm{e}^{\eta_-\mathrm{Tr}\,C}\int_{\mathbb{R}^4} dB'\ \exp\left[-\frac{1}{2}\eta_+\mathrm{Tr}\left(CC^T(B'B'^T)^{-1} + B'B'^T\right)\right]|\det B'|^{\nu-2}. \tag{3.14}$$

Note the similarity with eq. (3.3).

In a second step we perform the integral $\int dB'$. Because CC^T is a symmetric, positive definite matrix we can diagonalise it with an orthogonal transformation O

$$O^T(CC^T)O = \begin{pmatrix} \lambda_1 & 0 \\ 0 & \lambda_2 \end{pmatrix},\quad \lambda_{1,2} \geq 0\ . \tag{3.15}$$

Using the invariance of dB' we can change variables $B' \to OB'$ with $(B'B'^T)^{-1} \to O(B'B'^T)^{-1}O^T$. We thus replace CC^T by its diagonalised form eq. (3.15) in the exponent in eq. (3.14):

$$\mathrm{Tr}\left(B'B'^T + CC^T(B'B'^T)^{-1}\right) = a^2+b^2+c^2+d^2+h^{-2}((c^2+d^2)\lambda_1 + (a^2+b^2)\lambda_2), \tag{3.16}$$

where we have explicitly parametrised

$$B' \equiv \begin{pmatrix} a & b \\ c & d \end{pmatrix}, \; h \equiv \det B' = ad - bc \; . \tag{3.17}$$

We now introduce h as an independent variable in eq. (3.14) by inserting a delta-function constraint in its integral representation:

$$\begin{aligned} P(C) &= \frac{c_{N=2}\,\eta_+}{4\pi^4}\,\mathrm{e}^{\eta_-\mathrm{Tr}\,C}\int_{-\infty}^{\infty} dh\,|h|^{\nu-2}\int_{\mathbb{R}^4} dB'\int_{-\infty}^{\infty} d\omega\,\mathrm{e}^{-i\omega(h-(ad-bc))} \\ &\quad\times\exp\left[-\frac{\eta_+}{2}[a^2+b^2+c^2+d^2+h^{-2}((c^2+d^2)\lambda_1+(a^2+b^2)\lambda_2)]\right] \\ &= \frac{c_{N=2}\,\eta_+}{4\pi^4}\,\mathrm{e}^{\eta_-\mathrm{Tr}\,C}\,2\int_0^{\infty} dh\,h^{\nu-2}\int_{-\infty}^{\infty} d\omega\,\mathrm{e}^{-i\omega h}\frac{(2\pi)^2}{\omega^2+\eta_+^2(1+\lambda_1/h^2)(1+\lambda_2/h^2)}, \end{aligned} \tag{3.18}$$

where we performed the Gaussian integrals successively in pairs a, d and b, c, and switched to positive h. The denominator in the third line can be rewritten at the cost of an additional integral, $\frac{1}{a} = \int_0^{\infty} dt\,\mathrm{e}^{-at}$ for $a > 0$, and after changing variables $\omega \to \tau = \omega h$ we have

$$\begin{aligned} P(C) &= \frac{2c_{N=2}\,\eta_+}{\pi^2}\,\mathrm{e}^{\eta_-}\,\mathrm{Tr}\,C\int_0^{\infty} dh\,h^{\nu-1}\int_{-\infty}^{\infty} d\tau\,\mathrm{e}^{-i\tau}\int_0^{\infty} dt\,\mathrm{e}^{-(\tau^2+\eta_+^2(h^2+(\lambda_1+\lambda_2)+\lambda_1\lambda_2/h^2))t} \\ &= \frac{2c_{N=2}\,\eta_+}{\pi^{3/2}}\,(\lambda_1\lambda_2)^{\nu/4}\,\mathrm{e}^{\eta_-}\,\mathrm{Tr}\,C\int_0^{\infty}\frac{dt}{\sqrt{t}}\,\exp\left[-\eta_+^2(\lambda_1+\lambda_2)t-\frac{1}{4t}\right]\,K_{\frac{\nu}{2}}(2\eta_+^2\sqrt{\lambda_1\lambda_2}t). \end{aligned} \tag{3.19}$$

We performed the Gaussian integration over τ first, and then employed the following integral from [34] eq. 8.432.6

$$K_\nu(z) = \frac{1}{2}\,\left(\frac{z}{2}\right)^{\nu}\,\int_0^{\infty} dt\,\frac{\mathrm{e}^{-t-z^2/4t}}{t^{\nu+1}} \tag{3.20}$$

to do the h-integration after another change of variables, arriving at our result eq. (3.19).

As the final step we need to express $P(C)$ in terms of the eigenvalues of C (i.e. Λ_1^2 and Λ_2^2), rather than those of CC^T. This will also involve a Jacobian to be computed later. In eq. (3.19) we need

$$\mathrm{Tr}\,C = \Lambda_1^2+\Lambda_2^2\;, \qquad \lambda_1\lambda_2 = \det[CC^T] = \Lambda_1^4\Lambda_2^4\;, \tag{3.21}$$

which are trivial. Only the combination $\lambda_1+\lambda_2 = \mathrm{Tr}(CC^T)$ requires more calculation. In general, we can orthogonally transform any real matrix C to the form

$$C = \begin{pmatrix} \sin\theta & -\cos\theta \\ \cos\theta & \sin\theta \end{pmatrix}\begin{pmatrix} \epsilon_1 & s \\ -s & \epsilon_2 \end{pmatrix}\begin{pmatrix} \sin\theta & \cos\theta \\ -\cos\theta & \sin\theta \end{pmatrix} \tag{3.22}$$

where ϵ_1, ϵ_2, s and the rotation parameter θ are all real. The matrix parameters $\{\epsilon_1, \epsilon_2, s\}$ and eigenvalues $\{\Lambda_1^2, \Lambda_2^2\}$ follow from

$$0 = \begin{vmatrix} \epsilon_1-\Lambda^2 & s \\ -s & \epsilon_2-\Lambda^2 \end{vmatrix} = \Lambda^4-(\epsilon_1+\epsilon_2)\Lambda^2+(\epsilon_1\epsilon_2+s^2)\;, \tag{3.23}$$

with solution

$$\Lambda_{1,2}^2 = \frac{\epsilon_1+\epsilon_2}{2} \pm \sqrt{\frac{(\epsilon_1-\epsilon_2)^2}{4} - s^2}. \tag{3.24}$$

This can be inverted for $\epsilon_{1,2}$ for later use to

$$\epsilon_{1,2} = \frac{\Lambda_1^2+\Lambda_2^2}{2} \pm \sqrt{\frac{(\Lambda_1^2-\Lambda_2^2)^2}{4} + s^2}\ . \tag{3.25}$$

This immediately leads to

$$\lambda_1+\lambda_2 = \mathrm{Tr}(CC^T) = \epsilon_1^2+\epsilon_2^2+2s^2 = \Lambda_1^4+\Lambda_2^4+4s^2. \tag{3.26}$$

On inserting eqs. (3.21) and (3.26) into eq. (3.19) we can express $P(C)$ in terms of $\Lambda_{1,2}^2$. However, we have changed variables twice to arrive here, first from the matrix elements c_{ij} of C to $\{\epsilon_1,\epsilon_2,s,\theta\}$, and second from $\{\epsilon_1,\epsilon_2\}$ to $\{\Lambda_1^2,\Lambda_2^2\}$. The corresponding Jacobians we must multiply by are given by

$$\begin{aligned}\mathcal{J}_1 &= \left|\frac{\partial\{c_{11},c_{12},c_{21},c_{22}\}}{\partial\{\epsilon_1,\epsilon_2,s,\theta\}}\right| = 2\,|\epsilon_1-\epsilon_2|\,\cos^2(2\theta)\ ,\\ \mathcal{J}_2 &= \left|\frac{\partial\{\epsilon_1,\epsilon_2\}}{\partial\{\Lambda_1^2,\Lambda_2^2\}}\right| = \left|\frac{\Lambda_1^2-\Lambda_2^2}{\epsilon_1-\epsilon_2}\right|\ .\end{aligned} \tag{3.27}$$

3.2.1. Distinction of real and complex eigenvalues

In order to give the jpdf from eq. (3.19) for variables $\Lambda_{1,2}^2$ alone we have to integrate over the remaining real variables s and θ. Here we have to distinguish between the case of two real eigenvalues, and that of a complex conjugate pair. Starting from a real matrix C in eq. (3.22) all new variables, in particular $\epsilon_{1,2}$, are real. In view of eq. (3.25) there are two possibilities if the radicand is to remain positive:

(i) Λ_1^2,Λ_2^2 are both real $\Rightarrow \frac{1}{4}(\Lambda_1^2-\Lambda_2^2)^2+s^2\geq 0$ which is always satisfied, or
(ii) Λ_1^2,Λ_2^2 are complex conjugates: $\Lambda_1^2-\Lambda_2^2\in i\mathbb{R} \Rightarrow s^2\geq -\frac{1}{4}(\Lambda_1^2-\Lambda_2^2)^2\geq 0$.

We thus obtain for the jpdf

$$\begin{aligned}d\Lambda_1^2 d\Lambda_2^2 P(\Lambda_1^2,\Lambda_2^2) = \frac{2c_{N=2}\,\eta_+}{\pi^{3/2}}\,d\Lambda_1^2 d\Lambda_2^2\,\mathrm{e}^{\eta_-(\Lambda_1^2+\Lambda_2^2)}|\Lambda_1^2\Lambda_2^2|^{\nu/2}\int_0^{2\pi}d\theta\,\left|\Lambda_1^2-\Lambda_2^2\right|\cos^2(2\theta)\\ \times\ \int_{s_{min}}^{\infty}ds\,2\int_0^{\infty}\frac{dt}{\sqrt{t}}\exp\left[-\eta_+^2(\Lambda_1^4+\Lambda_2^4+4s^2)t-\frac{1}{4t}\right]K_{\frac{\nu}{2}}(2\eta_+^2|\Lambda_1^2\Lambda_2^2|t),\end{aligned} \tag{3.28}$$

where $s_{min}^2=\max\{0,-(\Lambda_1^2-\Lambda_2^2)^2/4\}$. The θ-integral is trivial.

For two real eigenvalues having $s_{min}=0$ the integral over s can be performed, leading to the following simplification for the remaining t-integral:

$$2\int_0^{\infty}\frac{dt}{t}\,\mathrm{e}^{-\eta_+^2(\Lambda_1^4+\Lambda_2^4)t-\frac{1}{4t}}K_{\frac{\nu}{2}}(2\eta_+^2|\Lambda_1^2\Lambda_2^2|t) = 2K_{\frac{\nu}{2}}(\eta_+|\Lambda_1^2|)\,2K_{\frac{\nu}{2}}(\eta_+|\Lambda_2^2|)\ . \tag{3.29}$$

Here we have used [34] eq. 6.653.2 after changing variables $t\to u=\frac{1}{2t}$. When ordering the two eigenvalues as $\Lambda_1^2>\Lambda_2^2$ the jpdf eq. (3.28) can thus be written as

$$P(\Lambda_1^2,\Lambda_2^2) = c_{N=2}\,(\Lambda_1^2-\Lambda_2^2)\prod_{j=1,2}|\Lambda_j^2|^{\nu/2}\mathrm{e}^{\eta_-\Lambda_j^2}\,2K_{\frac{\nu}{2}}(\eta_+|\Lambda_j^2|),\quad \Lambda_{1,2}^2\in\mathbb{R}\ , \tag{3.30}$$

as was claimed in eq. (2.9) in conjunction with eq. (2.13) for $N = 2$.

For two complex conjugate eigenvalues the s-integral leads to the complementary error function, without further simplification. Here we order $0 < \Im\mathrm{m}\Lambda_1^2 = -\Im\mathrm{m}\Lambda_2^2$ as in eq. (2.10) to obtain the following real, positive distribution

$$P(\Lambda_1^2,\Lambda_2^2)\,d\Lambda_1^2 d\Lambda_2^2 = c_{N=2}\,d\Lambda_1^2 d\Lambda_2^2\,(\Lambda_1^2-\Lambda_2^2)|\Lambda_1^2|^{\nu/2}|\Lambda_2^2|^{\nu/2}\mathrm{e}^{\eta_-(\Lambda_1^2+\Lambda_2^2)} \tag{3.31}$$
$$\times\, 2\int_0^\infty \frac{dt}{t}\,\mathrm{e}^{-\eta_+^2(\Lambda_1^4+\Lambda_2^4)t-\frac{1}{4t}}K_{\frac{\nu}{2}}(2\eta_+^2\Lambda_1^2\Lambda_2^2 t)\,\mathrm{erfc}(\eta_+\sqrt{t}\,|\Lambda_1^2-\Lambda_2^2|),\quad \Lambda_{1,2}^2\in\mathbb{C}\ .$$

Because the integral depends only on the modulus $|\Im\mathrm{m}\Lambda_1^2| = |\Im\mathrm{m}\Lambda_2^2|$ we can define its square root to be the weight of each eigenvalue Λ_j^2, as in eq. (2.14). The limit $|\Im\mathrm{m}\Lambda_1^2| \to 0$ smoothly reduces the integral in eq. (3.31) to eq. (3.29), using that $\mathrm{erfc}(0) = 1$.

Combining the real and complex cases, and still assuming the eigenvalue ordering, we can write the jpdf most generally as follows

$$d^2z_1 d^2z_2 P(z_1,z_2) = c_{N=2}\,d^2z_1 d^2z_2 (z_1-z_2)w(z_1)w(z_2) \tag{3.32}$$
$$\times\Big(\delta(y_1)\delta(y_2)\Theta(x_1-x_2) - 2i\delta^2(z_1-z_2^*)\Theta(y_1)\Big)$$

where we have switched variables $\Lambda^2 = z = x+iy$, including for the differentials, $d\Lambda^2 d\Lambda^{*\,2} = (dx+idy)(dx-idy) = -2idxdy = -2id^2z$. This is just the jpdf in eq. (2.9) including the weight eq. (2.12), and this completes our computation for the $N = 2$ case.

3.3. General structure for arbitrary N

In this subsection we will compute the jpdf for any N – both even and odd – given in terms of the eigenvalues Λ_j^2 of the Wishart matrix $C = AB^T$. We start from eq. (2.7) which we repeat here for convenience,

$$P(C) \sim \exp[\eta_-\mathrm{Tr}\,C]\int_{\mathbb{R}^{N(N+\nu)}} dA\int_{\mathbb{R}^{N(N+\nu)}} dB\ \exp\Big[-\frac{\eta_+}{2}\mathrm{Tr}(AA^T+BB^T)\Big]\,\delta(C-AB^T)\ . \tag{3.33}$$

We will eventually use the results from the previous two subsections as building blocks.

Instead of using a generalised Schur (or QZ) decomposition involving unitary matrices to bring A and B to upper triangular form, we will restrict ourselves here to orthogonal transformations. The best we can achieve in this way is a so-called almost (or quasi) upper triangular (AUT) form for one of the matrices, and an upper triangular form for the second (which is also AUT). An AUT matrix is composed of a block diagonal matrix, having non-vanishing 2×2 blocks along the diagonal for even N, and an additional 1×1 block at the end if N is odd. The remaining non-zero elements of an AUT matrix all lie above the block diagonal.

The precise transformation that we make is:

$$A = O_A(\Delta_A+\Lambda_A)O_B^T,\qquad B^T = O_B(\Delta_B+\Lambda_B)O_A^T. \tag{3.34}$$

Here Λ_A and Λ_B are block diagonal, and Δ_A and Δ_B are zero except in elements strictly above the block diagonal. $\Delta_A+\Lambda_A$ and $\Delta_B+\Lambda_B$ are hence AUT. Note that O_A is of size $N\times N$, and O_B is of size $(N+\nu)\times(N+\nu)$. Δ_A and Λ_A are each the same size as A itself (i.e. rectangular), and similarly Δ_B and Λ_B are the same size as B^T.

Matrix	Degrees of freedom	Matrix	Degrees of freedom	
			Even N	Odd N
A	$N(N+\nu)$	Λ_A	$2N$	$2N-1$
B	$N(N+\nu)$	Λ_B	$2N$	$2N-1$
		Δ_A	$\frac{N^2}{2}-N+\nu N$	$\frac{N^2+1}{2}-N+\nu N$
		Δ_B	$\frac{N^2}{2}-N$	$\frac{N^2+1}{2}-N$
		O_A	$\frac{N^2}{2}-N$	$\frac{N^2+1}{2}-N$
		O_B	$\frac{N^2}{2}-N+\nu N$	$\frac{N^2+1}{2}-N+\nu N$

Table 1. Counting dof before and after change of variables.

To make the transformation eq. (3.34) unique, having the same number of degrees of freedom (dof) on the left- and right-hand sides, we restrict O_A and O_B as follows:

$$\begin{aligned} &O_A \in O(N)/O(2)^{N/2}\,, \qquad O_B \in O(N+\nu)/O(2)^{N/2}\,O(\nu) \qquad \text{for even } N\,, \\ &O_A \in O(N)/O(2)^{(N-1)/2}\,,\ O_B \in O(N+\nu)/O(2)^{(N-1)/2}\,O(\nu) \qquad \text{for odd } N. \end{aligned} \tag{3.35}$$

The residual symmetries leading to these cosets are rotations within each block on the diagonal, and, loosely speaking, the extra factor $O(\nu)$ can be thought of as originating from the reduction of B from rectangular to square form, as in the $N=1$ and 2 cases earlier. The precise counting of dof is given in Table 1, matching the sum of dof of A and B for all N.

Under this orthogonal transformation, the integrand in eq. (2.7) changes as follows:

$$\exp\left[-\frac{\eta_+}{2}\mathrm{Tr}(AA^T+BB^T)\right] = \exp\left[-\frac{\eta_+}{2}\mathrm{Tr}(\Lambda_A\Lambda_A^T+\Lambda_B\Lambda_B^T+\Delta_A\Delta_A^T+\Delta_B\Delta_B^T)\right]. \tag{3.36}$$

The pre-factor $\exp\left[\eta_-\,\mathrm{Tr}C\right] = \exp\left[\eta_-\sum_{i=1}^N \Lambda_i^2\right]$ remains unchanged, with the relation between the eigenvalues Λ_i^2 and the new variables yet to be determined.

The transformation eq. (3.34) leads to the following differentials

$$\begin{aligned} (dA)_{ij} \;&= \Big(O_A[O_A^T dO_A(\Delta_A+\Lambda_A) - (\Delta_A+\Lambda_A)O_B^T dO_B + d\Delta_A + d\Lambda_A]O_B^T\Big)_{ij}, \\ (dB^T)_{ij} &= \Big(O_B[O_B^T dO_B(\Delta_B+\Lambda_B) - (\Delta_B+\Lambda_B)O_A^T dO_A + d\Delta_B + d\Lambda_B]O_A^T\Big)_{ij}. \end{aligned} \tag{3.37}$$

Here we have used the fact that for orthogonal transformations (with $O^TO=I$) the differential O^TdO is anti-symmetric. This remains true for our special choice of cosets. When considering the invariant line element $\mathrm{Tr}(dA\,dA^T + dB\,dB^T)$ the rotations outside the square brackets in eq. (3.37) can be dropped.

We will now compute the Jacobian for the change of variables from $\{dA, dB^T\}$ to $\{d\Lambda_A, d\Lambda_B, d\Delta_A, d\Delta_B, O_A^T dO_A, O_B^T dO_B\}$. Here we use the differentials for convenience as for the orthogonal matrices only these constitute independent variables (see also [31] for a similar discussion for the real Ginibre ensemble). In particular, counting dof $O_A^T dO_A$ is an anti-symmetric matrix with zeros not just on the diagonal but on the block diagonal. Similarly $O_B^T dO_B$ is an anti-symmetric matrix with zeros on the block diagonal for the first N elements, and a zero-block of size $\nu \times \nu$ on the remaining part of the diagonal.

In the differential eq. (3.37) the variables $\{d\Lambda_A, d\Lambda_B, d\Delta_A, d\Delta_B\}$ are already diagonal, with

$$\frac{\partial (dA)_{ij}}{\partial (d\Delta_A)_{pq}} = \delta_{ip}\delta_{jq} \ , \quad \frac{\partial (dA)_{ij}}{\partial (d\Lambda_A)_{pq}} = \delta_{ip}\delta_{jq} \ , \tag{3.38}$$

and similarly for dB^T. This contributes a unity matrix block to the Jacobi matrix $\mathcal{J}$, when considering the corresponding elements of $\{dA, dB^T\}$ on and above the block diagonal.

The non-trivial contribution from the Jacobian therefore originates from differentiating the remaining elements of $\{dA, dB^T\}$ below the block diagonal with respect to the independent variables of $\{O_A^T dO_A, O_B^T dO_B\}$, where we also choose the lower block diagonal elements for convenience. When appropriately ordering the elements of the Jacobi matrix (see Appendix A and also a similar discussion in [31]) the contributions proportional to Δ_A and Δ_B in eq. (3.37) will drop out, being part of a lower triangular sub-matrix in $\mathcal{J}$.

For the sake of argument we restrict ourselves in this section to the case of Λ_A and Λ_B being diagonal. The more general (and typical) case in which Λ_A and Λ_B contain 2×2 blocks is treated in Appendix A.

Arranging the remaining matrix elements below the block diagonal of dA and of the square part of dB^T into pairs this leads to a 2×2 block diagonal Jacobi sub-matrix with elements

$$\left| \det \begin{pmatrix} \frac{\partial (dA)_{ij}}{\partial (O_A^T dO_A)_{ij}} & \frac{\partial (dB)_{ij}}{\partial (O_A^T dO_A)_{ij}} \\ \frac{\partial (dA)_{ij}}{\partial (O_B^T dO_B)_{ij}} & \frac{\partial (dB)_{ij}}{\partial (O_B^T dO_B)_{ij}} \end{pmatrix} \right| = \left| \det \begin{pmatrix} (\Lambda_A)_{jj} & -(\Lambda_B)_{ii} \\ -(\Lambda_A)_{ii} & (\Lambda_B)_{jj} \end{pmatrix} \right| = |\Lambda_j^2 - \Lambda_i^2| \ , \tag{3.39}$$

where we used that $(\Lambda_A)_{jj}(\Lambda_B)_{jj} = \Lambda_j^2$ (no summations), and the Λ_j^2 are the eigenvalues of the matrix $C \equiv AB^T$. The remaining νN matrix elements below the block diagonal of dB^T give a diagonal sub-matrix with ν elements $(\Lambda_B)_{jj}$ each. The resulting contribution to the Jacobian is

$$\mathcal{J} = \prod_{1 \le i < j \le N}{}' |\Lambda_i^2 - \Lambda_j^2| \prod_{j=1}^{N} |(\Lambda_B)_{jj}|^\nu \ . \tag{3.40}$$

The prime on the product symbol denotes that only those factors with indices (i, j) strictly below the block diagonal are to be included. Finally, we observe that the second product can be written as

$$\prod_{j=1}^{N} |(\Lambda_B)_{jj}|^\nu = \begin{cases} \prod_{j=1}^{N/2} |\det B_j|^\nu & \text{for even } N, \\ \prod_{j=1}^{(N-1)/2} |\det B_j|^\nu |(\Lambda_B)_{NN}|^\nu & \text{for odd } N, \end{cases} \tag{3.41}$$

in which B_j is the j-th 2×2 block along the diagonal of the matrix Λ_B. The same statement is true in the more general case when Λ_A (and Λ_B) are not diagonal, as shown in Appendix A.

Writing everything together, we have for the total measure

$$\begin{aligned} &dA\,dB\ \mathrm{e}^{\eta_- \mathrm{Tr}\,AB^T - \frac{\eta_+}{2}\mathrm{Tr}(AA^T+BB^T)} \\ &\sim d\Lambda_A\,d\Lambda_B\,d\Delta_A\,d\Delta_B\,O_A^{-1}dO_A\,O_B^{-1}dO_B \prod_{1\le i<j\le N}{}' |\Lambda_i^2-\Lambda_j^2| \prod_{i=1}^N \mathrm{e}^{\eta_-\Lambda_i^2} \\ &\times \mathrm{e}^{-\frac{\eta_+}{2}\mathrm{Tr}(\Lambda_A^T\Lambda_A+\Lambda_B^T\Lambda_B+\Delta_A^T\Delta_A+\Delta_B^T\Delta_B)} \begin{cases} \prod_{j=1}^{N/2} |\det B_j|^\nu & \text{for even } N \\ \prod_{j=1}^{(N-1)/2} |\det B_j|^\nu |\Lambda_B|_{NN}^\nu & \text{for odd } N. \end{cases} \end{aligned} \tag{3.42}$$

All constant factors are omitted here; we give the overall normalisation constant later. We reiterate that B_j here is the j-th 2×2 block on the diagonal of Λ_B. The integration over the orthogonal dof as well as over the upper block triangular matrices $\Delta_{A,B}$ can now be performed as they decouple. The relevant dof for the right-hand side of eq. (3.42) can thus be written in terms of the Λ_i^2 and 2×2 blocks of the matrices $\Lambda_{A,B}$

$$\prod_{i<j}{}' |\Lambda_i^2-\Lambda_j^2| \begin{cases} \prod_{i=1}^{N/2} \left\{ dA_i\,dB_i\,\mathrm{e}^{\eta_-(\Lambda_{2i-1}^2+\Lambda_{2i}^2)} \mathrm{e}^{-\frac{\eta_+}{2}\mathrm{Tr}(A_i^TA_i+B_i^TB_i)} |\det B_i|^\nu \right\} & \text{for even } N, \\ \prod_{i=1}^{(N-1)/2} \{ \text{ ditto } \}_i\ da\,db\ \mathrm{e}^{\eta_-\Lambda_N^2} \mathrm{e}^{-\frac{\eta_+}{2}(a^2+b^2)} |b|^\nu & \text{for odd } N. \end{cases} \tag{3.43}$$

We have thus reduced the problem of computing the jpdf to a simpler problem involving only 2×2 and 1×1 blocks, which can be handled just as the $N=2$ and $N=1$ cases that we treated in the previous two subsections. For this, it is necessary to order the eigenvalues as described in eq. (2.10). Then, following eq. (3.32), each 2×2 block will make the following contribution in variables $\Lambda_i^2 = z_i$ (with Λ_{2i-1}^2 and Λ_{2i}^2 either both real or complex conjugates, and ordered as described at the end of Section 3.2)

$$\begin{aligned} &d^2z_{2i-1}\,d^2z_{2i}(z_{2i-1}-z_{2i})w(z_{2i-1})w(z_{2i}) \\ &\times \Big(\delta(y_{2i-1})\delta(y_{2i})\Theta(x_{2i-1}-x_{2i}) - 2i\delta^2(z_{2i-1}-z_{2i}^*)\Theta(y_{2i-1})\Big)\,. \end{aligned} \tag{3.44}$$

In a similar way, we have for the 1×1 block when N is odd

$$d^2z_N\,|z_N|^{\nu/2}\,\mathrm{e}^{\eta_- z_N}\,g(z_N)\,\delta(y_N) = d^2z_N w(z_N)\,\delta(y_N)\,, \tag{3.45}$$

where z_N will be real. Note that collecting all these quantities in eq. (3.43) for each $i=1$ to $[N/2]$ the factors $\Lambda_{2i-1}^2-\Lambda_{2i}^2$ will combine with the $\prod_{i<j}'(\Lambda_i^2-\Lambda_j^2)$ to make a true Vandermonde determinant $\prod_{i<j}(\Lambda_i^2-\Lambda_j^2)$, and we were able to drop the modulus sign because of the chosen ordering. The final answer for the jpdf is therefore as claimed in eq. (2.9). The normalisation constant can be determined by keeping track of all volume factors and μ-dependencies; it is given by

$$c_N = (VO(N)2^{-N}(2\pi)^{-N(N+1)/4})^2(2\pi)^{-N\nu/2}\,\frac{VO(N+\nu)}{VO(N)VO(\nu)}(2\mu)^{-N(N+\nu)}\eta_+^{-N(N+\nu-1)/2}. \tag{3.46}$$

4. Finite- and large-N density correlation functions

4.1. The kernel

The kernel $\mathcal{K}_N(z_1, z_2)$ as it initially appears in eq. (2.18) is *defined* as follows [7]

$$\mathcal{K}_N(z_1, z_2) \equiv \sum_{k=1}^{N} \sum_{l=1}^{N} \mathcal{A}^{-1}_{kl} z_1^{k-1} z_2^{l-1} \tag{4.1}$$

where the matrix $\mathcal{A}$ of dressed moments is related to $\mathcal{F}$ by

$$\mathcal{A}_{kl} \equiv \int d^2z_1\, d^2z_2\, \mathcal{F}(z_1, z_2)\, z_1^{k-1} z_2^{l-1}. \tag{4.2}$$

However, to evaluate the matrix $\mathcal{A}$ and its inverse directly is not trivial in general. Fortunately, the kernel may also be derived from the expectation value of the product of two characteristic polynomials [20]

$$H_N(\lambda, \gamma) \equiv \langle \det(\lambda - \mathcal{D})\, \det(\gamma - \mathcal{D}^T) \rangle_N, \tag{4.3}$$

where $\mathcal{D}$ was given in eq. (2.2). An explicit form for $H_N(\lambda, \gamma)$ was derived by the authors in [20].[+] In the case of the real Ginibre ensemble the spectral density was known prior to its integrability [4] and thus was used for the determination of the kernel in [7].

To establish the relationship between $\mathcal{K}_N(z_1, z_2)$ and $H_{N-2}(\lambda, \gamma)$, we first relate the latter to the complex eigenvalue density $R^{\mathbb{C}}_{1,N}(z)$. If we choose $\gamma = \lambda^*$ with $\Im\mathrm{m}\, \lambda^2 > \Im\mathrm{m}\, \gamma^2$ we have

$$\begin{aligned} H_{N-2}(\lambda, \lambda^*) &= \int_{\mathbb{C}} d^2z_1 \ldots \int_{\mathbb{C}} d^2z_{N-2} P_{N-2}(z_1, \ldots, z_{N-2}) (\lambda\lambda^*)^\nu \prod_{j=1}^{N-2} (\lambda^2 - z_j^2)(\lambda^{*\,2} - z_j^2) \\ &= \frac{c_{N-2}}{c_N} \frac{1}{\exp[-\eta_-(\lambda^2 + \lambda^{2\,*})] g(\lambda^2)^2 (\lambda^2 - \lambda^{2\,*})(-2i)\Theta(\Im\mathrm{m}\lambda^2)} \\ &\quad \times \int_{\mathbb{C}} d^2z_1 \ldots \int_{\mathbb{C}} d^2z_{N-2} \tilde{P}_N(z_1, \ldots, z_{N-2}, \lambda^2, \lambda^{2\,*}) \,, \end{aligned} \tag{4.4}$$

where $\tilde{P}_N$ indicates that this jpdf is conditioned that the last two eigenvalues are complex conjugates and ordered. The last line in eq. (4.4) is thus nothing but the complex density $R^{\mathbb{C}}_{1,N}(\lambda^2)$, obtained by inserting a delta function into the partition function together with the constraint that the last two eigenvalues are complex conjugates. We thus arrive at the following relationship

$$R^{\mathbb{C}}_{1,N}(z) = \frac{c_N}{c_{N-2}} \frac{w(z) w(z^*)}{|z|^\nu} (-2i)(z - z^*)\, H_{N-2}(\sqrt{z}, \sqrt{z^*}). \tag{4.5}$$

On the other hand we have from eq. (2.25) an equation that relates the complex density directly to the kernel

$$R_{1,N}(z) = \int_{\mathbb{C}} d^2u\, \mathcal{K}_N(z, u)\, \mathcal{F}(u, z) \tag{4.6}$$

[+] Note that P and Q were called A and B in [20]; we set n in [20] to unity here.

and so for complex z inserting eq. (2.19)

$$R^{\mathbb{C}}_{1,N}(z) = \mathcal{K}_N(z, z^*)\, w(z)w(z^*)(-2i)\ \mathrm{sgn}(y). \tag{4.7}$$

We can therefore make the identification (after analytic continuation in each argument)

$$\mathcal{K}_N(u, v) = \frac{c_N}{c_{N-2}}(u - v)\, \frac{H_{N-2}(\sqrt{u}, \sqrt{v})}{(uv)^{\nu/2}}. \tag{4.8}$$

Using the solution for $H_N(\lambda, \gamma)$ obtained in [20] as well as eq. (3.46), we then have for the properly normalised kernel that

$$\mathcal{K}_N(u, v) = \frac{\eta_-}{8\pi(4\mu^2\eta_+)^{\nu+1}} \sum_{j=0}^{N-2} \left(\frac{\eta_-}{\eta_+}\right)^{2j} \frac{(j+1)!}{(j+\nu)!} \left\{ L^\nu_{j+1}\left(\frac{v}{4\mu^2\eta_-}\right) L^\nu_j\left(\frac{u}{4\mu^2\eta_-}\right) \right.$$
$$\left. - L^\nu_{j+1}\left(\frac{u}{4\mu^2\eta_-}\right) L^\nu_j\left(\frac{v}{4\mu^2\eta_-}\right) \right\}, \tag{4.9}$$

which is the same as eq. (2.20). It can be further simplified to be expressed as an anti-symmetric derivative as follows. For modified Laguerre polynomials, we can use a recurrence relation to show that

$$\begin{aligned}(j+1)\left\{L^\nu_{j+1}(y)L^\nu_j(x) - (x \leftrightarrow y)\right\} &= \left(y\frac{\partial}{\partial y}L^\nu_j(y) + (j+\nu+1-y)L^\nu_j(y)\right) L^\nu_j(x) \\ &\quad - (x \leftrightarrow y) \\ &= \left(y\frac{\partial}{\partial y} - x\frac{\partial}{\partial x} - (y-x)\right) L^\nu_j(x)L^\nu_j(y). \end{aligned} \tag{4.10}$$

The kernel therefore becomes

$$\mathcal{K}_N(z_1, z_2) = \frac{\eta_-}{8\pi(4\mu^2\eta_+)^{\nu+1}} \left(y\frac{\partial}{\partial y} - x\frac{\partial}{\partial x} - (y-x)\right) \sum_{j=0}^{N-2} \left(\frac{\eta_-}{\eta_+}\right)^{2j} \frac{j!}{(j+\nu)!} L^\nu_j(x)L^\nu_j(y) \tag{4.11}$$

where x and y are evaluated at $x = z_1/4\mu^2\eta_-$ and $y = z_2/4\mu^2\eta_-$ after the differentiations. The symmetric kernel in terms of Laguerre polynomials on the right hand side of eq. (4.11) is nothing else but the kernel of the complex ($\beta = 2$) two-matrix model [16].

We have explicitly checked that a similar relation holds relating the kernel of the non-chiral real Ginibre ensemble (see the equation after 5.26 in second ref. [8]) to $(\partial_y - \partial_x - 2(y-x))$ operating on the kernel of the non-chiral complex Ginibre ensemble (see eq. 40 in [32]) and thus this is a more general feature.

Note that the convention used in [20] for defining the 'kernel' was different from that adopted here (in eq. (4.9)); in that paper, there was no division by $(uv)^{\nu/2}$, and the summation ran to N. There was also a minor typographical error in the arguments of one function (eq. 33 in [20]).

4.2. Finite-N results

From eq. (2.18) we have

$$R_1(z_1) = \int_{\mathbb{C}} d^2z\, \mathcal{K}_N(z_1, z)\mathcal{F}(z, z_1) \equiv R^{\mathbb{C}}_1(z_1) + \delta(y_1)R^{\mathbb{R}}_1(x_1)\ . \tag{4.12}$$

We now simply insert the finite-N kernel eq. (4.9) and weight function eq. (2.12) into this using eq. (2.19), to give

$$R_1^{\mathbb{C}}(z) = -2i\ \mathrm{sgn}(\Im m\, z)\ 2\int_0^\infty \frac{dt}{t} \mathrm{e}^{-\eta_+^2 t(z^2+z^{*\,2})-\frac{1}{4t}} K_{\frac{\nu}{2}}\left(2\eta_+^2 t|z|^2\right) \mathrm{erfc}\left(2\eta_+\sqrt{t}|\Im m\, z|\right)$$
$$\times \frac{\eta_-|z|^\nu \mathrm{e}^{2\eta_-\Re \mathrm{e}\, z}}{8\pi(4\mu^2\eta_+)^{\nu+1}} \sum_{j=0}^{N-2}\left(\frac{\eta_-}{\eta_+}\right)^{2j} \frac{(j+1)!}{(j+\nu)!}\left\{L_{j+1}^\nu\left(\frac{z^*}{4\mu^2\eta_-}\right) L_j^\nu\left(\frac{z}{4\mu^2\eta_-}\right) - \text{c.c.}\right\} \tag{4.13}$$

$$R_1^{\mathbb{R}}(x) = \frac{\eta_-}{8\pi(4\mu^2\eta_+)^{\nu+1}} \int_{-\infty}^\infty dx' \mathrm{sgn}(x-x')|xx'|^{\nu/2} \mathrm{e}^{\eta_-(x+x')} 2K_{\frac{\nu}{2}}(\eta_+|x|) 2K_{\frac{\nu}{2}}(\eta_+|x'|)$$
$$\times \sum_{j=0}^{N-2}\left(\frac{\eta_-}{\eta_+}\right)^{2j} \frac{(j+1)!}{(j+\nu)!}\left\{L_{j+1}^\nu\left(\frac{x'}{4\mu^2\eta_-}\right) L_j^\nu\left(\frac{x}{4\mu^2\eta_-}\right) - (x' \leftrightarrow x)\right\}. \tag{4.14}$$

These results are valid for even N only. Alternatively we could have used the form eq. (4.11) which is more reminiscent of the corresponding chGOE result [35] at $\mu = 0$. In fact we have checked that in the limit $\mu \to 0$ the complex density eq. (4.13) vanishes, and the real density eq. (4.14) reduces to the finite-N expression (equation 5.18 in [35]) for the chGOE, after using some identities for modified Laguerre polynomials. We have also checked these results numerically using Monte Carlo, by generating random matrices and explicitly diagonalising them.

As the last step we can change from squared variables $z = x + iy = \Lambda^2$ to Dirac eigenvalues Λ, using eq. (2.28). These two densities are illustrated* in Figures 1 and 2, showing the localisation of the support for finite N.

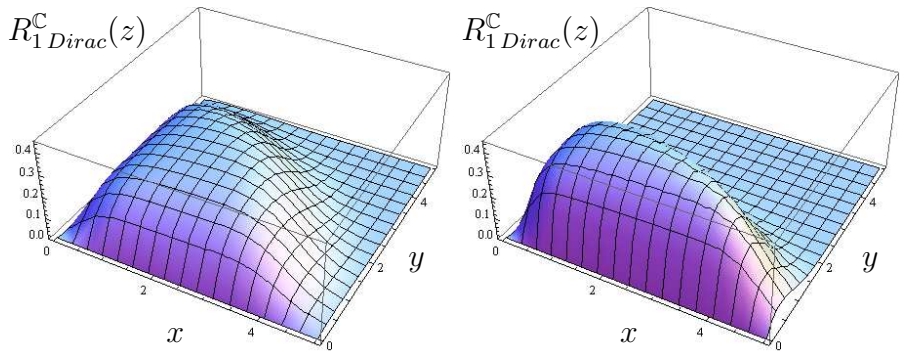

Figure 1. The complex spectral density $R_{1\,Dirac}^{\mathbb{C}}(z)$ for finite $N = 10$ at maximal non-Hermiticity $\mu^2 = 1$ (left) and intermediate $\mu^2 = 0.5$ (right), both for $\nu = 0$. We show only the first quadrant for symmetry reasons. For $\mu = 1$ we see a circular "support" growing with $\sqrt{N}$, apart from the repulsion from the axes. For decreasing μ the "support" becomes an ellipse, with the eigenvalues moving towards, as well as onto, the real axis. Note the increased height in the right plot.

* Here and in the following numerical integrals are carried out using [36].

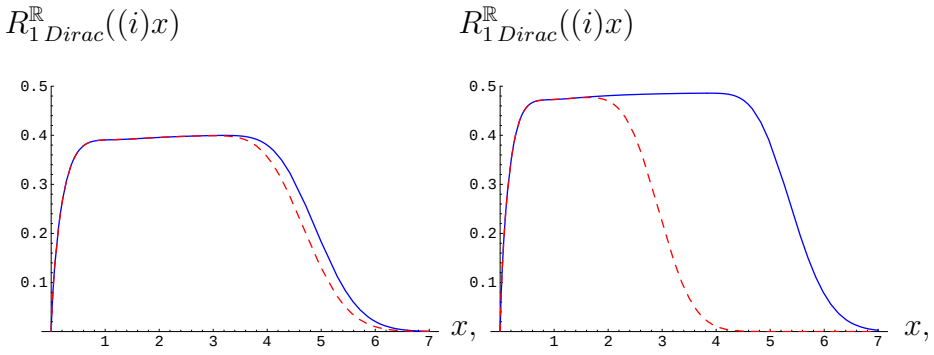

Figure 2. The spectral density $R^{\mathbb{R}}_{1\,Dirac}(x)$ for real eigenvalues (blue full line) and $R^{\mathbb{R}}_{1\,Dirac}(ix)$ for purely imaginary eigenvalues (red dashed line) for finite $N = 10$ at almost maximal non-Hermiticity $\mu^2 = 0.95$ (left) and intermediate $\mu^2 = 0.5$ (right), both for $\nu = 0$. Here we have chosen (almost) the same parameter values as Fig. 1, with $\mu^2 = 0.95$ here close to 1 there. Because of chiral symmetry real and imaginary eigenvalues come in $\pm$ pairs and we only have to show the positive axes, comparing both distributions in the same plot. Whilst for $\mu^2 = 0.95$ the distributions of real and imaginary Dirac eigenvalues are almost the same, for $\mu^2 = 0.5$ there are more eigenvalues on the real than on the imaginary axis.

4.3. The large-N limit at strong non-Hermiticity

In the strong non-Hermitian limit, we keep μ fixed as we take the large-N limit. This necessitates *no* rescaling of the eigenvalues (see Section 2), which is why our result is also true away from the origin. Let us first determine the large-N limit of the kernel.

Reference [34] eq. 8.976.1 gives us the so-called Hille-Hardy formula (the equivalent of Mehler's formula for Hermite polynomials):

$$S(x,y,z) \equiv \sum_{j=0}^{\infty} \frac{j!}{(j+\nu)!} L_j^{\nu}(x) L_j^{\nu}(y) z^j = \frac{(xyz)^{-\nu/2}}{1-z} \mathrm{e}^{-\frac{z}{1-z}(x+y)} I_{\nu}\left(\frac{2\sqrt{xyz}}{1-z}\right). \tag{4.15}$$

We can insert this into eq. (4.11) and evaluate it after extending the sum to infinity. On differentiating the right-hand side, certain terms cancel, and we can therefore establish that

$$y\,\frac{\partial S(x,y,z)}{\partial y} - x\,\frac{\partial S(x,y,z)}{\partial x} = -\frac{z}{1-z}\,(y-x)\,S(x,y,z). \tag{4.16}$$

Hence the limit as $N \to \infty$ of the kernel is easily seen to be

$$\mathcal{K}_{\nu}^{S}(z_1,z_2) \equiv \lim_{N\to\infty} \mathcal{K}_N(z_1,z_2) = \frac{\eta_+^3}{8\pi}(z_1-z_2)\,\mathrm{e}^{-\eta_-(z_1+z_2)}\,(z_1 z_2)^{-\nu/2}\,I_{\nu}\left(2\eta_+\sqrt{z_1 z_2}\right). \tag{4.17}$$

Because of this simplification this is now *proportional* to the $\beta = 2$ kernel at strong non-Hermiticity. Multiplication by the weight function eq. (2.12) which contains the modulus $|z_1 z_2|^{\nu/2}$ will only cancel the pre-factor in eq. (4.17) up to a phase. Putting all ingredients together we can determine the eigenvalue densities using eq. (2.25):

$$\rho_\nu^{\mathbb{C}\,S}(z) = \mathrm{sgn}(\Im m\, z)(-2i)(z-z^*)\frac{\eta_+^3}{8\pi} I_\nu\left(2\eta_+|z|\right) \tag{4.18}$$
$$\times\, 2\int_0^\infty \frac{dt}{t}\, \exp\left[-\eta_+^2(z^2+z^{*\,2})t - \frac{1}{4t}\right]\, K_{\frac{\nu}{2}}\left(2\eta_+^2|z|^2 t\right)\, \mathrm{erfc}\left(2\eta_+\sqrt{t}\,|\Im m\, z|\right),$$

$$\rho_\nu^{\mathbb{R}\,S}(x) = \frac{\eta_+^3}{8\pi}\, 2K_{\frac{\nu}{2}}(\eta_+|x|)\left(\int_0^\infty dx'\,|x-x'|\; 2K_{\frac{\nu}{2}}(\eta_+|x'|)\; I_\nu(2\eta_+\sqrt{xx'})\right. \tag{4.19}$$
$$\left. + \int_{-\infty}^0 dx'\,|x-x'|\; 2K_{\frac{\nu}{2}}(\eta_+|x'|)\; J_\nu(2\eta_+\sqrt{x|x'|})\right).$$

Note the change from Bessel-I to Bessel-J function inside the integral for negative arguments, after taking into account the aforementioned phase.

If we rescale the eigenvalues as $2\eta_+ z^2 \to z^2$ (and divide the densities by $2\eta_+$ accordingly) we obtain the same densities as at maximal non-Hermiticity. These are obtained by setting $\mu = 1 \Rightarrow \eta_+ = \frac{1}{2}$ above, or by starting from the kernel eq. (2.30) at maximal non-Hermiticity. This feature that the strong limit can be obtained by rescaling the case of maximal non-Hermiticity is generically true for complex RMT, see [30].

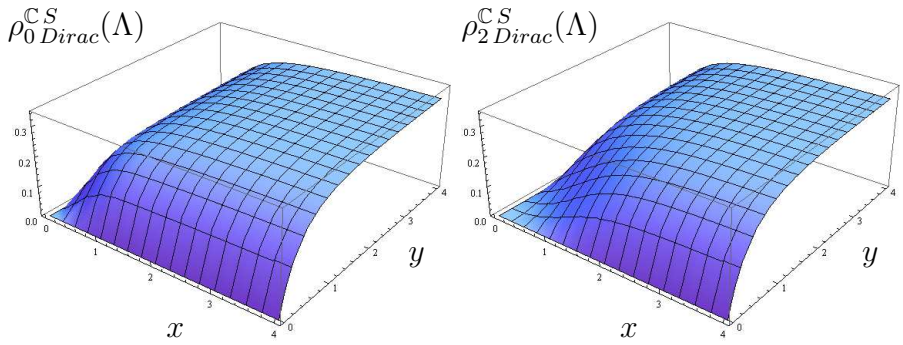

Figure 3. The complex spectral density $\rho_{\nu\,Dirac}^{\mathbb{C}\,S}(\Lambda = x+iy)$ at maximal non-Hermiticity $\mu = 1$. It is shown only in the first quadrant for symmetry reasons, for $\nu = 0$ (left) and $\nu = 2$ (right). Increasing the number of exact zero eigenvalues ν leads to a stronger repulsion from the origin. At $\nu = 0$ this repulsion is still present due to chiral symmetry (or technically speaking the presence of the Bessel-K function).

In Figures 3 and 4 we show the densities of Dirac eigenvalues Λ for complex eigenvalues and real or purely imaginary eigenvalues respectively, using the mapping eq. (2.28). Because of the rescaling property just mentioned we only show results here for maximal non-Hermiticity. One can check analytically using a saddle-point approximation including the fluctuations that for asymptotically large x, y the densities eqs. (4.18) and (4.19) decay as $\sim 1/|z|$ and $1/\sqrt{x}$ respectively. After the mapping to Dirac eigenvalues eq. (2.28) they thus reach a plateau as seen in the figures. We note that the profiles of the densities on the real and imaginary axis are very reminiscent to parallel cuts through the complex densities, for both values of ν shown.

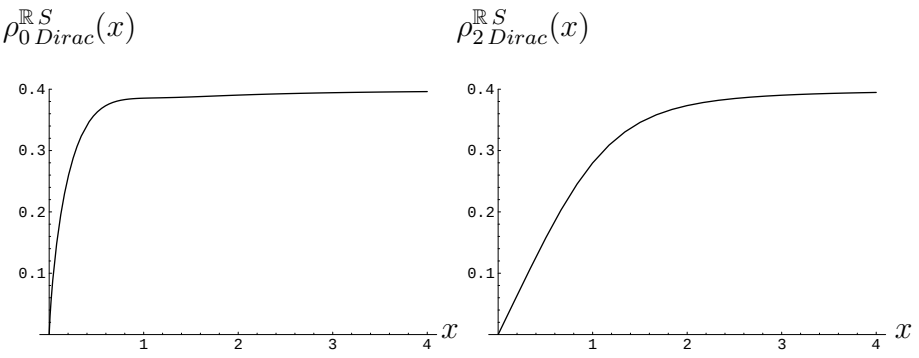

Figure 4. The real spectral density of Dirac eigenvalues on the positive half-line at maximal non-Hermiticity $\mu = 1$ for $\nu = 0$ (left) and $\nu = 2$ (right). Because of chiral symmetry it is symmetric on the negative real line, and because $\mu = 1$ it is identical on the imaginary axis. For $\nu = 2$ we see the increased repulsion from the origin compared to $\nu = 0$, as for the complex eigenvalues in Fig. 3.

4.4. The large-N limit at weak non-Hermiticity

In the weak case, we scale μ and z with N as follows (as compared with the unscaled case, i.e. we implicitly include here the first rescaling discussed in Section 2.4)

$$\mu \equiv \frac{\alpha}{\sqrt{2N}} \ , \quad 4Nz \equiv \hat{z} \tag{4.20}$$

where α and $\hat{z}$ are kept fixed throughout. Because of the rescaling of the eigenvalues here we are magnifying the region around the origin.

For the weight function we thus simply obtain

$$\lim_{N\to\infty} K_{\frac{\nu}{2}}\left(\eta_+ \frac{|z|}{4N}\right) = K_{\frac{\nu}{2}}\left(\frac{|z|}{8\alpha^2}\right) \quad \text{and} \quad \lim_{N\to\infty} \exp\left[\eta_- \frac{z}{4N}\right] = \exp\left[\frac{z}{8\alpha^2}\right]. \tag{4.21}$$

For the kernel we are interested in the limit of eq. (4.9) in terms of the rescaled variables, i.e. μ, η_- and η_+ which all now depend on N. Instead of using eq. (4.11) it is slightly simpler if we can rewrite eq. (4.9) so that the Laguerre polynomials inside the sum are of the same degree j. Using the recurrence relationship for the Laguerre polynomials (eq. 8.971.2 in [34]), we have

$$\begin{aligned}(n+1)\left\{L_{n+1}^{\nu}(v)\, L_n^{\nu}(u) - (u \leftrightarrow v)\right\} &= \left((n+1+\nu)L_n^{\nu}(v) - vL_n^{\nu+1}(v)\right) L_n^{\nu}(u) - (u \leftrightarrow v) \\ &= uL_n^{\nu+1}(u)\, L_n^{\nu}(v) - vL_n^{\nu+1}(v)\, L_n^{\nu}(u) \ . \end{aligned} \tag{4.22}$$

The kernel can therefore be written as

$$\begin{aligned}\mathcal{K}_N(z_1, z_2) \ = \ & \frac{1}{8\pi(4\mu^2\eta_+)^{\nu+1}4\mu^2} \sum_{j=0}^{N-2} \left(\frac{\eta_-}{\eta_+}\right)^{2j} \frac{j!}{(j+\nu)!} \\ & \times \left\{ z_1 L_j^{\nu+1}\left(\frac{z_1}{4\mu^2\eta_-}\right) L_j^{\nu}\left(\frac{z_2}{4\mu^2\eta_-}\right) - z_2 L_j^{\nu+1}\left(\frac{z_2}{4\mu^2\eta_-}\right) L_j^{\nu}\left(\frac{z_1}{4\mu^2\eta_-}\right)\right\}. \end{aligned} \tag{4.23}$$

We now wish to take the limit $N \to \infty$. For this to exist we must multiply the kernel by the spacing as well as by the appropriate number of zero-eigenvalues from the weight, as given in eq. (4.27) below. In eq. (4.23) we will replace the sum with an integral over

the variable $t \equiv \frac{j}{N} \in [0,1]$. Because of the different scaling in the weak limit we cannot use the Hille-Hardy formula as before.

In detail, using eq. 8.978.2 in [34] we have for some real constant ν and fixed $t \in [0,1]$ the standard Bessel asymptotic of the modified Laguerre polynomials:

$$\lim_{N\to\infty} \left[N^{-\nu}\, L^{\nu}_{tN}\left(\frac{x}{N}\right)\right] = t^{\nu/2} x^{-\nu/2}\, J_\nu(2\sqrt{xt}). \tag{4.24}$$

We also have (keeping t fixed so that $j = tN \to \infty$)

$$\lim_{N\to\infty} \left(\frac{1-\frac{\alpha^2}{2N}}{1+\frac{\alpha^2}{2N}}\right)^{2j} = \exp[-2\alpha^2 t] \quad \text{and} \quad \lim_{N\to\infty} \frac{j!}{(j+\nu)!}\, N^{\nu} = t^{-\nu}. \tag{4.25}$$

Therefore,

$$\begin{aligned}
\mathcal{K}^W(z_1,z_2) \equiv & \lim_{N\to\infty} \left[\frac{1}{(4N)^2} \left(\frac{z_1 z_2}{(4N)^2}\right)^{\nu/2} \mathcal{K}_N\left(\frac{z_1}{4N}, \frac{z_2}{4N}; \mu = \frac{\alpha}{\sqrt{2N}}\right)\right] && (4.26)\\
= & \frac{1}{256\pi\alpha^2} \int_0^1 ds\, s^2\, \mathrm{e}^{-2\alpha^2 s^2} \left\{ \sqrt{z_1}\, J_{\nu+1}(s\sqrt{z_1}) J_\nu(s\sqrt{z_2}) - (z_1 \leftrightarrow z_2)\right\} && (4.27)\\
= & \frac{1}{128\pi\alpha^2} \left(z_2 \frac{\partial}{\partial z_2} - z_1 \frac{\partial}{\partial z_1}\right) \int_0^1 ds\; s\; \mathrm{e}^{-2\alpha^2 s^2} J_\nu\left(s\sqrt{z_1}\right) J_\nu\left(s\sqrt{z_2}\right)
\end{aligned}$$

after a simple change of variables in the integral. In the last line we expressed the kernel as a derivative of the $\beta = 2$ kernel at weak non-Hermiticity. This corresponds to eq. (4.11) in which the second term $-(y-x)$ now becomes sub-leading compared with the derivatives. The same relation between the large-N kernel at weak non-Hermiticity is true for the $\beta = 1$ and $\beta = 2$ Ginibre ensembles [8, 32] respectively.

Collecting all elements we have for the complex density

$$\begin{aligned}
\rho^{\mathbb{C}\,W}_{\nu}(z) = & -2i\, \mathrm{sgn}(\Im\mathrm{m}\, z) \exp\left[\frac{1}{8\alpha^2} 2\,\Re\mathrm{e}\, z\right] \mathcal{K}^W(z, z^*) && (4.28)\\
& \times 2 \int_0^\infty \frac{dt}{t} \exp\Big[-\frac{t}{64\alpha^4}(z^2 + z^{*\,2}) - \frac{1}{4t}\Big] K_{\frac{\nu}{2}}\left(\frac{t}{32\alpha^4}|z|^2\right) \mathrm{erfc}\Big(\frac{\sqrt{t}}{4\alpha^2}|\Im\mathrm{m}\, z|\Big).
\end{aligned}$$

In Figure 5 it is shown after mapping to Dirac eigenvalues. As a consistency check we can take the limit $\alpha \to \infty$ while keeping z/α^2 fixed to obtain once more the complex density in the strong non-Hermiticity limit, eq. (4.18). The precise mapping of weak to strong eigenvalues is given by $\frac{z}{4\alpha^2} \to 2\eta_+ z$. Whilst the matching of the integrals over t is straightforward the mapping of the kernels multiplied by the weight is more involved. Changing variables we have the following identity:

$$\begin{aligned}
& \alpha^2 \int_0^1 ds\, s^2\, \mathrm{e}^{-2\alpha^2 s^2} \left\{ \sqrt{z_1} J_{\nu+1}(s\sqrt{z_1}) J_\nu(s\sqrt{z_2}) - (z_1 \leftrightarrow z_2)\right\}\\
= & \; 2 \left(z_2 \frac{\partial}{\partial z_2} - z_1 \frac{\partial}{\partial z_1}\right) \int_0^\alpha dt\; t\; \mathrm{e}^{-2t^2} J_\nu\left(t\frac{\sqrt{z_1}}{\alpha}\right) J_\nu\left(t\frac{\sqrt{z_2}}{\alpha}\right)\\
\to & \; \frac{1}{2} \left(z_2 \frac{\partial}{\partial z_2} - z_1 \frac{\partial}{\partial z_1}\right) \exp\left[-\frac{(z_1+z_2)}{8\alpha^2}\right] I_\nu\left(\frac{\sqrt{z_1 z_2}}{4\alpha^2}\right)
\end{aligned} \tag{4.29}$$

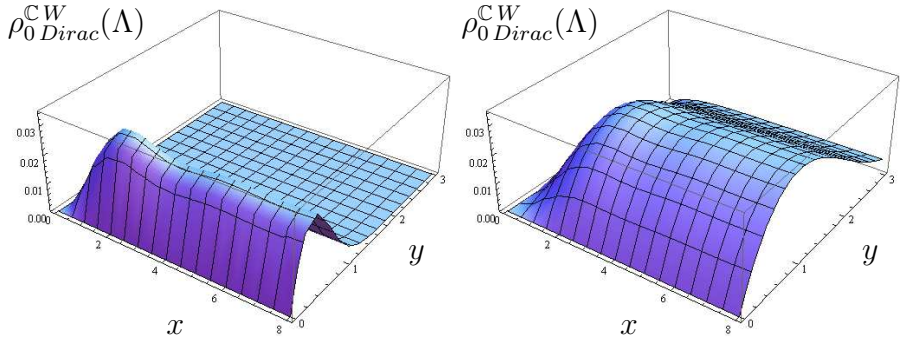

Figure 5. The complex spectral density $\rho_{\nu\ Dirac}^{\mathbb{C}\,W}(\Lambda = x+iy)$ at weak non-Hermiticity for parameters $\alpha^2 = 0.2$ (left) and $\alpha^2 = 1$ (right), both at $\nu = 0$ plotted on the same scale. For increasing α more complex eigenvalues move in towards the imaginary axis, reaching Fig. 3 left in the limit $\alpha \to \infty$.

where in the last step we have extended the integral to infinity and used eq. 6.633.2 [34]. The last differentiation is trivial, in effect acting only on the exponential function. We thus obtain for the limiting kernel

$$\lim_{\alpha\to\infty} \alpha^4 \mathcal{K}^W(z_1, z_2)\Big|_{\frac{z}{\alpha^2}\ \text{fixed}} = \left(\frac{z_1}{4\alpha^2} - \frac{z_2}{4\alpha^2}\right) \exp\left[-\frac{(z_1+z_2)}{8\alpha^2}\right] I_\nu\left(\frac{\sqrt{z_1 z_2}}{4\alpha^2}\right), \tag{4.30}$$

which precisely cancels the exponentials from the weight eq. (4.21) to arrive at the complex density at strong non-Hermiticity eq. (4.18).

We now turn to the real density at weak non-Hermiticity. Looking at the definitions eqs. (4.13) and (4.14) the main difference to the complex density is that here the kernel is integrated, whereas the complex density is simply given by the kernel multiplied by the weight.

Unfortunately, and in contrast to the strong non-Hermitian case, at weak non-Hermiticity the large-N limit and the integration do *not* commute, with the integral over the weak kernel (4.27) not being absolutely convergent. Such a feature might have been expected, as the same phenomenon occurs for the chGOE at $\mu = 0$ [35]. However, in that case, the integrals could be computed exactly before taking the large-N limit, leading to the correct result, which differs from the naive limit by a factor of 2 in the normalisation♯. The integrals in eq. (4.14) at finite N are more involved, and this matter will be addressed in future work.

For that reason we show in Fig. 6 the real density for finite but large $N = 10$ and 20, using the weak scaling from eq. (4.26) and eq. (4.20) for a given α. This underlines that the weak limit for the real density does exist and convergence is rapid. Furthermore we have checked this by superimposing data for $N = 100$ using numerically generated random matrices.

As a feature common to the strong limit we note that the densities of real and purely imaginary eigenvalues in Fig. 6 resemble cuts through the complex density in Fig. 5 left at the same value of $\alpha^2 = 0.2$.

♯ A quick guess generalising this to our setting fails.

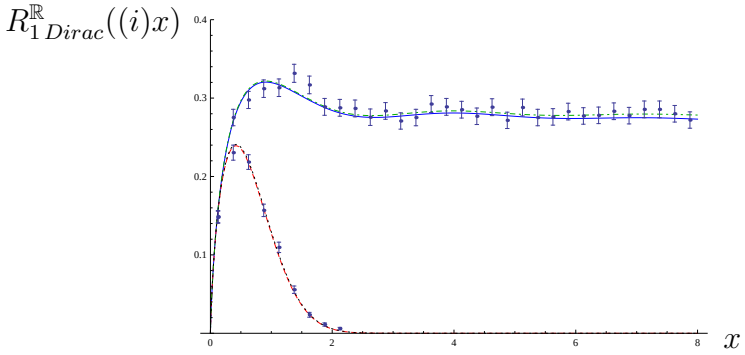

Figure 6. The real spectral density of Dirac eigenvalues on the positive half-line scaled as for weak non-Hermiticity for $\alpha^2 = \mu^2/2N = 0.2$ at $\nu = 0$. We show results for finite N vs numerical simulations. Both the eigenvalue densities for real eigenvalues $R^{\mathbb{R}}_{1,Dirac}(x)$ and for pure imaginary ones $R^{\mathbb{R}}_{1,Dirac}(ix)$ are displayed in the same plot for comparison. Real density: $N = 10$ (blue full line), $N = 20$ (dark green dot-dashed line); imaginary density $N = 10$ (red dashed line) $N = 20$ (black, dotted line). Dots with error bars: $N = 100$ Monte Carlo simulation of 10^4 matrices.

5. Conclusions

In this paper we have solved the chiral extension of the Ginibre ensemble of real asymmetric matrices. It is given as a two-matrix model of rectangular matrices with real elements and depends on a non-Hermiticity parameter μ. This model is relevant for computing the non-Hermitian spectrum of Dirac operators with real elements in field theory. Our work completes the programme of solving the three chiral or Wishart-Laguerre counterparts of the classical Ginibre ensembles, where earlier works by Osborn and one of the authors extended the models with complex and quaternion real elements respectively.

Whilst our model inherits most of the integrable structure of the real Ginibre ensemble its joint probability distribution required a more complicated calculation, which took much of our effort here. Just as in the Ginibre ensembles the probability density for the matrix elements is Gaussian, whereas the one for the eigenvalues becomes non-Gaussian. It contains a Bessel-K function and integral thereof, replacing the role of the complementary error function in the real Ginibre ensemble.

The main building block for all eigenvalue correlation functions is given by a kernel of Laguerre polynomials in the complex plane and was derived in a previous paper. Here, we give all eigenvalue density correlation functions for finite (even) N valid for all values of μ, in particular the spectral one-point densities for real eigenvalues and for complex non-real eigenvalues. Moreover, we have uncovered a way of expressing the $\beta = 1$ kernel in terms of the $\beta = 2$ kernel at finite and large N, both for the chiral and non-chiral Ginibre ensembles. We conjecture that a similar relation holds for the $\beta = 4$ kernel as well.

When taking microscopic large-N limits we focus on the origin where the chiral symmetry of our model is the most important. For both the limit at strong non-

Hermiticity with $0 < \mu^2 < 1$, and the limit at weak non-Hermiticity with $\mu^2 \sim 1/N$, we give compact expressions for the kernel. This leads to explicit expressions for the complex spectral one-point densities and the real density at strong non-Hermiticity.

It would be very interesting to compare these results with simulations from non-Hermitian lattice gauge theory, as was successfully done previously for the other two chiral two-matrix models.

Further extensions would be to investigate the bulk or the soft edge scaling limit. We expect that in the former the chiral ensembles will agree with the Ginibre ensembles, as the effect of chirality becomes unimportant in the bulk.

This work has been supported partly by European Network ENRAGE MRTN-CT-2004-005616 (G.A.), an EPSRC doctoral training grant (M.J.P.) and the SFB/TR12 of the Deutsche Forschungsgemeinschaft (H.-J.S.). We thank Tilo Wettig for useful discussions.

Appendix A. Details on the calculation of the Jacobian

In this appendix we give a few more details to complete the computation of the Jacobian from Section 3.3. In particular we first give a precise ordering of matrix elements leading to a block-triangular Jacobian. Second we will treat the case of non-diagonal matrices Λ_A and Λ_B.

For the first purpose we repeat eq. (3.37) including matrix indices, after dropping the outside rotations:

$$\begin{aligned}(dA)_{ij} &= \sum_{k=1}^{N}(O_A^T dO_A)_{ik}(\Delta_A+\Lambda_A)_{kj} - \sum_{k=1}^{N+\nu}(\Delta_A+\Lambda_A)_{ik}(O_B^T dO_B)_{kj} \\ &\quad + (d\Delta_A)_{ij} + (d\Lambda_A)_{ij}\ , \qquad (A.1)\\ (dB^T)_{ij} &= \sum_{k=1}^{N+\nu}(O_B^T dO_B)_{ik}(\Delta_B+\Lambda_B)_{kj} - \sum_{k=1}^{N}(\Delta_B+\Lambda_B)_{ik}(O_A^T dO_A)_{kj} \\ &\quad + (d\Delta_B)_{ij} + (d\Lambda_B)_{ij}\ . \qquad (A.2)\end{aligned}$$

We now give an ordering leading to a block-triangular Jacobi matrix, with variables $\{dA, dB^T\}$ in the columns and $\{d\Lambda_A, d\Lambda_B, d\Delta_A, d\Delta_B, O_A^T dO_A, O_B^T dO_B\}$ in the rows. For the block diagonal matrices $\Lambda_{A,B}$ and upper block-diagonal matrices $\Delta_{A,B}$ (of different size) this is trivial: we just group them together with the corresponding elements of dA and dB^T. For example, when N is even and $\nu > 0$, this will give

$$\begin{aligned}&(dA)_{11}, (dA)_{12}, (dA)_{21}, (dA)_{22}, (dA)_{33}, \ldots, (dA)_{NN}, (dB^T)_{11}, \ldots, (dB^T)_{NN}, (dA)_{13}, \\ &(dA)_{14}, \ldots, (dA)_{1,N+\nu}, (dA)_{23}, \ldots, (dA)_{N,N+\nu}, (dB^T)_{13}, \ldots, (dB^T)_{N-2,N} \qquad (A.3)\end{aligned}$$

versus

$$\begin{aligned}&(d\Lambda_A)_{11}, (d\Lambda_A)_{12}, (d\Lambda_A)_{21}, (d\Lambda_A)_{22}, (d\Lambda_A)_{33}, .., (d\Lambda_A)_{NN}, (d\Lambda_B)_{11}, .., (d\Lambda_B)_{NN}, (d\Delta_A)_{13}, \\ &(d\Delta_A)_{14}, \ldots, (d\Delta_A)_{1,N+\nu}, (d\Delta_A)_{23}, \ldots, (d\Delta_A)_{N,N+\nu}, (d\Delta_B)_{13}, \ldots, (d\Delta_B)_{N-2,N}\ . \qquad (A.4)\end{aligned}$$

The resulting sub-Jacobi matrix is clearly the identity matrix, and the order we have picked is arbitrary as long as we pair $(dA)_{ij}$ with $(d\Lambda_A)_{ij}$ or $(d\Delta_A)_{ij}$, and respectively for B.

It remains to order the matrix elements dA and dB^T below the block diagonal. In order to obtain sub-blocks as in eq. (3.39) we will always pair $(dA)_{ij}$ with the square part of $(dB^T)_{ij}$, with $i > j$ and $i, j \in 1, \ldots, N$ and finish with the rectangular part of $(dB^T)_{ij}$, with $i = N+1, \ldots, N+\nu$. For that we write the following partial differentials denoted by "|" from eqs. (A.1) and (A.2)

$$(dA|)_{i>j} \equiv \sum_{p=1}^{p<j<i} (O_A^T dO_A)_{ip}(\Delta_A)_{pj} - \sum_{q>i>j}^{N+\nu} (\Delta_A)_{iq}(O_B^T dO_B)_{qj} \ , \tag{A.5}$$

$$(dB^T|)_{i>j} \equiv \sum_{p=1}^{p<j<i} (O_B^T dO_B)_{ip}(\Delta_B)_{pj} - \sum_{q>i>j}^{N} (\Delta_B)_{iq}(O_A^T dO_A)_{qj} \ . \tag{A.6}$$

Here we have already used that $\Lambda_{A,B}$ are upper triangular, and that $i > j$ lets only the independent elements of the orthogonal differentials appear (we have chosen the below block diagonal ones).

For the variables $\Delta_{A,B}$ below the block diagonal, in order not to interfere with the block diagonals eq. (3.39), we introduce the following ordering of elements:

$$\begin{aligned} &(i,j) \prec (i,p) \text{ if } p < j \ , \\ &(i,j) \prec (q,j) \text{ if } q > i \ . \end{aligned} \tag{A.7}$$

Here $\prec$ implies that the matrix element (i,j) on the left, that is $(dA)_{ij}$ $((O_A^T dO_A)_{ij})$ has to appear before the one on the right ††. Looking back to eqs. (A.5) and (A.6) this implies that the elements $(dA)_{ij}$ and $(dB^T)_{ij}$ that depend on the most elements of $(O_A^T dO_A)_{ij}$ and $(O_B^T dO_B)_{ij}$ will appear first, leading to a lower triangular structure. However, the ordering eq. (A.7) is not unique. We will proceed 2×2 block-wise (plus 1×2 blocks for the last row when N is odd) going down the diagonal, in order to preserve the block-diagonal structure when the matrices $\Lambda_{A,B}$ are not diagonal.

We thus continue the labelling in eqs. (A.3) and (A.4) as

$$\begin{aligned} &(dA)_{32}, (dB^T)_{32}, (dA)_{31}, (dB^T)_{31}, (dA)_{42}, (dB^T)_{42}, (dA)_{41}, (dB^T)_{41}, (dA)_{54}, (dB^T)_{54}, \ldots, \\ &(dA)_{N1}, (dB^T)_{N1} \end{aligned} \tag{A.8}$$

versus

$$\begin{aligned} &(O_A^T dO_A)_{32}, (O_B^T dO_B)_{32}, (O_A^T dO_A)_{31}, (O_B^T dO_B)_{31}, (O_A^T dO_A)_{42}, (O_B^T dO_B)_{42}, (O_A^T dO_A)_{41}, \\ &(O_B^T dO_B)_{41}, (O_A^T dO_A)_{54}, (O_B^T dO_B)_{54}, \ldots, (O_A^T dO_A)_{N1}, (O_B^T dO_B)_{N1} \ . \end{aligned} \tag{A.9}$$

It remains for us to order the rectangular part of $(dB^T)_{ij}$ with $i = N+1, \ldots, N+\nu$ vs the corresponding $(O_B^T dO_B)_{ij}$. Using the same order as in eq. (A.7) we complete our Jacobi matrix by

$$(dB^T)_{N+1,N}, (dB^T)_{N+1,N-1}, \ldots, (dB^T)_{N+1,1}, (dB^T)_{N+2,N}, \ldots, (dB^T)_{N+\nu,1} \tag{A.10}$$

†† Our ordering is different from appendix A.37 in [31] for the real Ginibre ensemble.

versus

$$(O_B^T dO_B)_{N+1,N}, (O_B^T dO_B)_{N+1,N-1}, \ldots, (O_B^T dO_B)_{N+1,1}, (O_B^T dO_B)_{N+2,N}, \ldots,$$
$$(O_B^T dO_B)_{N+\nu,1} \ . \tag{A.11}$$

In the second part of this appendix we will deal with the case of $\Lambda_{A,B}$ being 2×2 block matrices rather than diagonal, which was omitted in Section 3.3. We start with N even, and first only deal with the matrix elements dA and the square part of dB^T below the block diagonal (eqs. (A.8) and (A.9)). In this case it is no longer sufficient to study one pair of neighbouring elements as in eq. (3.39), but rather four pairs. This leads to the following 8×8 matrix with the order chosen above: In the columns we put $(dA)_{i,j+1}, (dB^T)_{i,j+1}, (dA)_{ij}, (dB^T)_{ij}, (dA)_{i+1,j+1}, (dB^T)_{i+1,j+1}, (dA)_{i+1,j}, (dB^T)_{i+1,j}$, and in the rows the elements $(O_A^T dO_A)_{ij}$ and $(O_B^T dO_B)_{ij}$ in the corresponding order. Using eqs. (A.1) and (A.2) this leads to the following sub-matrices down the diagonal for each odd i and odd j:

$$\begin{pmatrix}
(\Lambda_A)_{j+1,j+1} & -(\Lambda_B)_{ii} & (\Lambda_A)_{j+1,j} & 0 & 0 & -(\Lambda_B)_{i+1,i} & 0 & 0 \\
-(\Lambda_A)_{ii} & (\Lambda_B)_{j+1,j+1} & 0 & (\Lambda_B)_{j+1,j} & -(\Lambda_A)_{i+1,i} & 0 & 0 & 0 \\
(\Lambda_A)_{j,j+1} & 0 & (\Lambda_A)_{jj} & -(\Lambda_B)_{ii} & 0 & 0 & 0 & -(\Lambda_B)_{i+1,i} \\
0 & (\Lambda_B)_{j,j+1} & -(\Lambda_A)_{ii} & (\Lambda_B)_{jj} & 0 & 0 & -(\Lambda_A)_{i+1,i} & 0 \\
0 & -(\Lambda_B)_{i,i+1} & 0 & 0 & (\Lambda_A)_{j+1,j+1} & -(\Lambda_B)_{i+1,i+1} & (\Lambda_A)_{j+1,j} & 0 \\
-(\Lambda_A)_{i,i+1} & 0 & 0 & 0 & -(\Lambda_A)_{i+1,i+1} & (\Lambda_B)_{j+1,j+1} & 0 & (\Lambda_B)_{j+1,j} \\
0 & 0 & 0 & -(\Lambda_B)_{i,i+1} & (\Lambda_A)_{j,j+1} & 0 & (\Lambda_A)_{jj} & -(\Lambda_B)_{i+1,i+1} \\
0 & 0 & -(\Lambda_A)_{i,i+1} & 0 & 0 & (\Lambda_B)_{j,j+1} & -(\Lambda_A)_{i+1,i+1} & (\Lambda_B)_{jj}
\end{pmatrix} \tag{A.12}$$

We can easily verify (using the symbolic manipulation capabilities of Mathematica [36], for example) that the modulus of the determinant of this is identical to

$$\mathcal{J}_{ij} = \Big|(D_i - D_j)^2 + (S_i - S_j)(S_i D_j - S_j D_i)\Big| \tag{A.13}$$

in which D_i is the determinant, and S_i the trace, of the 2×2 matrix U_i given by (only relevant for odd i)

$$U_i \equiv \begin{pmatrix} (\Lambda_A)_{ii} & (\Lambda_A)_{i,i+1} \\ (\Lambda_A)_{i+1,i} & (\Lambda_A)_{i+1,i+1} \end{pmatrix} \begin{pmatrix} (\Lambda_B)_{ii} & (\Lambda_B)_{i,i+1} \\ (\Lambda_B)_{i+1,i} & (\Lambda_B)_{i+1,i+1} \end{pmatrix}. \tag{A.14}$$

The same definition obviously applies for subscript j. However, D_i and S_i can of course be written in terms of the eigenvalues of U_i, which we denoted Λ_i^2 and Λ_{i+1}^2, i.e.

$$D_i = \det U_i = \Lambda_i^2 \Lambda_{i+1}^2 \ , \quad S_i = \mathrm{Tr}\, U_i = \Lambda_i^2 + \Lambda_{i+1}^2. \tag{A.15}$$

Substituting these into eq. (A.13), and factorising, gives

$$\mathcal{J}_{ij} = \Big|(\Lambda_i^2 - \Lambda_j^2)(\Lambda_{i+1}^2 - \Lambda_j^2)(\Lambda_i^2 - \Lambda_{j+1}^2)(\Lambda_{i+1}^2 - \Lambda_{j+1}^2)\Big|. \tag{A.16}$$

This is exactly what we got in the case when the Λ_A and Λ_B matrices were diagonal, i.e. the product of four copies of eq. (3.39), one for each of the combinations (i, j), $(i+1, j)$, $(i, j+1)$ and $(i+1, j+1)$.

When N is odd, we can treat the 2×2 blocks up to $N-1$ (inclusive) as before. We still have to consider the final column of dA, etc., and it is necessary here to treat (j, N)

and $(j+1, N)$ together as 2×1 blocks (for odd values of j in the range $1 \leq j < N$). Hence, we have extra diagonal blocks in the Jacobian (for each odd j) of the form

$$\begin{pmatrix} (\Lambda_A)_{j+1,j+1} & -(\Lambda_B)_{NN} & (\Lambda_A)_{j+1,j} & 0 \\ -(\Lambda_A)_{NN} & -(\Lambda_B)_{j+1,j+1} & 0 & (\Lambda_B)_{j+1,j} \\ (\Lambda_A)_{j,j+1} & 0 & (\Lambda_A)_{jj} & -(\Lambda_B)_{NN} \\ 0 & (\Lambda_B)_{j,j+1} & -(\Lambda_A)_{NN} & (\Lambda_B)_{jj} \end{pmatrix} \tag{A.17}$$

which is in fact the first sub-block of eq. (A.12) with $i = N$. The modulus of the determinant of this is identically equal to

$$\mathcal{J}_{Nj} = \left| D_j - S_j \Lambda_N^2 + \Lambda_N^4 \right|, \tag{A.18}$$

where we used that $(\Lambda_A)_{NN}(\Lambda_B)_{NN} = \Lambda_N^2$ (no sums), and D_j and S_j were defined as before. But we can switch to writing D_j and S_j in terms of the eigenvalues of U_j, and this gives

$$\mathcal{J}_{Nj} = \left| (\Lambda_N^2 - \Lambda_j^2)(\Lambda_N^2 - \Lambda_{j+1}^2) \right|. \tag{A.19}$$

We see that this is again of the expected form.

Let us turn to the remaining variables, the rectangular part of dB^T in eqs. (A.10) and (A.11). We first suppose that N is even. For each i and each odd j we find that the variables $(dB^T)_{i,j+1}, (dB^T)_{ij}$ and $(O_B^T dO_B)_{i,j+1}, (O_B^T dO_B)_{ij}$ are now coupled into the following 2×2 blocks:

$$\begin{pmatrix} (\Lambda_B)_{j+1,j+1} & (\Lambda_B)_{j+1,j} \\ (\Lambda_B)_{j,j+1} & (\Lambda_B)_{jj} \end{pmatrix} \tag{A.20}$$

whose determinant is (after a relabelling $2j-1 \to j$) simply $\det B_j$ (using the definition of B_j after eq. (3.41)). This is independent of i which takes ν different values, $N+1 \leq i \leq N+\nu$. We therefore have a total contribution to the Jacobian of

$$\prod_{j=1}^{N/2} |\det B_j|^\nu \text{ for } N \text{ even}, \tag{A.21}$$

which is exactly as before (eq. (3.41)).

Finally, when N is odd, we just pick up an extra factor of $(\Lambda_B)_{NN}$ from each of the ν cells in the last column $(dB^T)_{iN}$, and so

$$\prod_{j=1}^{(N-1)/2} |\det B_j|^\nu |(\Lambda_B)_{NN}|^\nu \text{ for } N \text{ odd}. \tag{A.22}$$

This ends the calculation for non-diagonal matrices $\Lambda_{A,B}$.

References

[1] J. Ginibre, J. Math. Phys. **6**, 440 (1965).

[2] Y.V. Fyodorov and H.-J. Sommers, J. Phys. **A**: Math. Gen. **36** (2003) 3303 [arXiv:nlin.CD/0207051].

[3] N. Lehmann and H.-J. Sommers, Phys. Rev. Lett. **67**, 941 (1991).

[4] A. Edelman, J. Multivariate Anal. **60**, 203 (1997).

[5] E. Kanzieper and G. Akemann, Phys. Rev. Lett. **95**, 230201 (2005) [arXiv:math-ph/0507058]; G. Akemann and E. Kanzieper, J. Stat. Phys. **129**, 1159 (2007) [arXiv:math-ph/0703019].

[6] C.D. Sinclair, Int. Math. Res. Not. **2007** rnm015 (2007) [arXiv:math-ph/0605006].

[7] H.-J. Sommers, J. Phys. **A40**, F671 (2007) [arXiv:0706.1671].

[8] P.J. Forrester and T. Nagao, Phys. Rev. Lett. **99** 050603 (2007) [arXiv:0706.2020 [cond-mat.stat-mech]]; J. Phys. **A41**, 375003 (2008) [arXiv:0806.0055 [math-ph]]

[9] A. Borodin and C.D. Sinclair, arXiv:0706.2670v2 [math-ph]; arXiv:0805.2986 [math-ph].

[10] H.-J. Sommers and W. Wieczorek, J. Phys. **A41**, 405003 (2008) [arXiv:0806.2756 [cond-mat.stat-mech]].

[11] P.J. Forrester and A. Mays, arXiv:0809.5116v2 [math-ph]

[12] E.V. Shuryak and J.J.M. Verbaarschot, Nucl. Phys. **A560** (1993) 306 [arXiv:hep-th/9212088]; J. Verbaarschot, Phys. Rev. Lett. **72** (1994) 2531 [arXiv:hep-th/9401059v1].

[13] M.A. Stephanov, Phys. Rev. Lett. **76** (1996) 4472. [arXiv:hep-lat/9604003].

[14] M.A. Halasz, J.C. Osborn, and J.J.M. Verbaarschot, Phys. Rev. **D56** (1997) 7059 [arXiv:hep-lat/9704007].

[15] K. Splittorff and J.J.M. Verbaarschot, Nucl. Phys. **B683** (2004) 467 [arXiv:hep-th/0310271v3]

[16] J.C. Osborn, Phys. Rev. Lett. **93** (2004) 222001 [arXiv:hep-th/0403131].

[17] G. Akemann, J. Phys. **A**: Math. Gen. **36** (2003) 3363 [arXiv:hep-th/0204246].

[18] G. Akemann, J.C. Osborn, K. Splittorff, and J.J.M. Verbaarschot, Nucl. Phys. **B712** (2005) 287. [arXiv:hep-th/0411030].

[19] G. Akemann, Nucl. Phys. **B730**, 253 (2005) [arXiv:hep-th/0507156]; G. Akemann and F. Basile, Nucl. Phys. **B766**, 150 (2007) [arXiv:math-ph/0606060].

[20] G. Akemann, M.J. Phillips, and H.-J. Sommers, J. Phys. **A**: Math. Theor. **42** (2009) 012001 [arXiv:0810.1458v1 [math-ph]].

[21] J.J.M. Verbaarschot, Les Houches Summer School, France, 6-25 June 2004, arXiv:hep-th/0502029v1;
G. Akemann, Int. J. Mod. Phys. **A22** (2007) 1077 [arXiv:hep-th/0701175].

[22] D. Bernard and A. LeClair, *A Classification of Non-Hermitian Random Matrices*, proceedings of the NATO Advanced Research Workshop on Statistical Field Theories, Como 18-23 June 2001, [arXiv:cond-mat/0110649];
U. Magnea, J. Phys. **A41**, 045203 (2008) [arXiv:0707.0418v2 [math-ph]].

[23] P.J. Forrester and A. Mays, arXiv:0910.2531 [math-ph]

[24] A. Edelman, E. Kostlan, and M. Shub, J. Amer. Math. Soc. **7**, 247 (1994).

[25] G. Akemann and G. Vernizzi, Nucl. Phys. **B660**, 532 (2003) [arXiv:hep-th/0212051].

[26] C.A. Tracy and H. Widom, J. Stat. Phys. **92** (1998) 809.

[27] P.J. Forrester, T. Nagao, and G. Honner, Nucl. Phys. **B553** (1999) 601 [arXiv:cond-mat/9811142v1 [cond-mat.mes-hall]].

[28] K.B. Efetov, Phys. Rev. Lett. **79** 491 (1997) [arXiv:cond-mat/9702091 [cond-mat.dis-nn]].

[29] H.-J. Sommers, A. Crisanti, H. Sompolinsky, and Y. Stein, Phys. Rev. Lett **60** (1988) 1895.

[30] Y.V. Fyodorov, B.A. Khoruzhenko, and H.-J. Sommers, Ann. Inst. Henri Poincaré **68**, 449 (1998) [arXiv:chao-dyn/9802025].

[31] M.L. Mehta, *Random Matrices*, Academic Press, Third Edition, London (2004).

[32] Y.V. Fyodorov, B.A. Khoruzhenko, and H.-J. Sommers, Phys. Lett. **A226** (1997) 46 [arXiv:cond-mat/9606173]; Phys. Rev. Lett. **79** (1997) 557 [arXiv:cond-mat/9703152].

[33] M. Abramowitz and I.E. Stegun, *Handbook of Mathematical Functions*, Dover Publications Inc., New York (1965).

[34] I.S. Gradshteyn and I.M. Ryzhik, *Table of Integrals, Series and Products*, 6th Edition, Academic Press, London (2000).

[35] J. Verbaarschot, Nucl. Phys. **B426** (1994) 559 [arXiv:hep-th/9401092v1].

[36] Wolfram Research, Inc., *Mathematica*, Version 7.0, Champaign, IL (2008)